Table 2
Dosimetric results for the intraoperative dosimetry, the Day 1 and Day 30 postimplant dosimetry

		Mean	SD	Min	Max	Difference	95% CI		p-Value
Prostate									
pD_{90} (%)	Intraop	133.7	11.0	95.2	160.0				
	Day 1	115.6	12.2	81.1	149.9	19.91	17.1	22.7	<0.001
	Day 30	125.8	18.5	82.9	178.1	7.0	3.7	10.4	<0.001
pV_{100} (%)	Intraop	98.0	2.2	87.6	100.0				
	Day 1	93.9	6.0	58.6	100.0	4.1	3.1	5.2	<0.001
	Day 30	96.9	4.1	78.0	100.0	1.6	0.7	2.4	<0.001
pV_{150} (%)	Intraop	72.9	11.4	31.1	94.4				
	Day 1	55.5	13.5	10.8	89.9	18.8	16.1	21.4	<0.001
	Day 30	68.6	16.5	23.4	98.8	5.4	2.5	8.3	<0.001
Volume (mL)	Intraop	31.4	7.9	11.9	53.3				
	Day 1	32.1	9.2	13.1	59.5	−0.57	−1.7	0.5	0.313
	Day 30	26.0	7.8	11.4	46.6	5.37	4.0	6.8	<0.001
Urethra									
uD_{90} (%)	Intraop	122.0	17.6	80.0	209.7				
	Day 1	96.4	18.7	34.8	140.0	25.6	21.8	29.4	<0.001
	Day 30	117.3	22.1	69.9	178.6	3.9	−0.8	8.6	0.103
uD_{30} (%)	Intraop	152.7	17.3	106.2	238.6				
	Day 1	140.3	18.5	99.3	223.4	17.7	14.5	21.0	<0.001
	Day 30	186.0	27.4	139.3	264.8	−23.8	−33.9	−13.8	<0.001
Rectum									
rV_{100} (mL)	Intraop	0.69	0.64	0.00	2.7				
	Day 1	0.46	0.54	0.00	2.7	0.3	0.1	0.4	0.002
	Day 30	1.02	0.95	0.00	4.6	0.3	−0.5	−0.1	0.002
rV_{150} (mL)	Intraop	0.04	0.09	0.00	0.6				
	Day 1	0.04	0.09	0.00	0.5	0.0	0.0	0.0	0.832
	Day 30	0.12	0.21	0.00	1.3	−0.1	−0.1	0.0	0.001

SD = standard deviation; Min = minimum; Max = maximum; CI = confidence interval; pD_{90} = dose covering 90% of prostate volume; intraop = intraoperative; pV_{100} = prostate volume covered by 100% of the prescription dose; pV_{150} = prostate volume covered by 150% of the prescription dose; uD_{90} = dose covering 90% of the urethra; uD_{30} = dose covering 30% of the urethra; rV_{100} = rectal volume covered by 100% of the prescription dose; rV_{150} = rectal volume covered by 150% of the prescription dose.

or linear regression analysis were performed. Differences were regarded as statistically significant at the $p < 0.05$ level.

Results

Comparison of intraoperative and Day 1 and Day 30 parameters

Dosimetric data from all 160 patients are summarized in Table 2. Data indicated a general good quality of implantation using US-based dosimetry, with pD_{90} being >100% of the prescribed dose and V_{100} covering >95% of the prostate. However, significant differences were seen between US and CT in most dosimetric parameters.

Regarding prostate parameters, mean pD_{90} on intraoperative US, CT_1, and CT_{30} were 133.7%, 115.6%, and 125.8% of the prescribed dose, respectively. pD_{90} temporarily decreased on CT_1 and increased on CT_{30} but did not overtake the initial value on intraoperative US. Other parameters, such as pV_{100} and pV_{150} showed similar trends. Prostate volume tended to be slightly increased on CT_1 and significantly decreased on CT_{30} compared with intraoperative US.

Regarding urethral parameters, mean uD_{90} on intraoperative US, CT_1, and CT_{30} were 122.0%, 96.4%, and 117.3% of the prescribed dose, respectively. The uD_{90} value temporarily decreased on CT_1 and increased on CT_{30} to the same level as intraoperative US. A similar trend was seen with uD_{30} but that value overtook the initial value on intraoperative US.

Regarding rectal parameters, mean rV_{100} on intraoperative US, CT_1, and CT_{30} were 0.69, 0.46, and 1.02 mL, respectively. The rV_{100} value temporarily decreased on CT_1 and increased on CT_{30} to a level higher than that of intraoperative US. Mean V_{150} showed almost the same trend.

Generally, we tended to overestimate prostate and urethral parameters on US relative to CT-based dosimetry. Conversely, we tended to underestimate rectal parameters on US relative to CT-based dosimetry.

Correlations between intraoperative and Day 1 and Day 30 parameters

A positive linear relationship was present between US and CT observations for every prostate parameter

(Table 3). In addition, uD_{30} also showed a positive linear relationship between US and CT. Although associations were not strong, these correlation factors might be useful to predict CT-based dosimetry.

Table 3
Correlation coefficient of CT dosimetry to intraoperative US dosimetry

		Correlation coefficient	*p*-Value
Prostate			
pD_{90} (%)	Day 1	0.18	0.072
	Day 30	0.34	<0.001
pV_{100} (%)	Day 1	0.42	<0.001
	Day 30	0.23	0.022
pV_{150} (%)	Day 1	0.36	<0.001
	Day 30	0.51	<0.001
Urethra			
uD_{90} (%)	Day 1	0.11	0.165
	Day 30	0.14	0.123
uD_{30} (%)	Day 1	0.53	<0.001
	Day 30	0.46	0.021
Rectum			
rV_{100} (mL)	Day 1	−0.04	0.672
	Day 30	−0.02	0.788
rV_{150} (mL)	Day 1	−0.10	0.284
	Day 30	−0.01	0.961

CT = computed tomography; US = ultrasonography; pD_{90} = dose covering 90% of prostate volume; pV_{100} = prostate volume covered by 100% of the prescription dose; pV_{150} = prostate volume covered by 150% of the prescription dose; uD_{90} = dose covering 90% of the urethra; uD_{30} = dose covering 30% of the urethra; rV_{100} = rectal volume covered by 100% of the prescription dose; rV_{150} = rectal volume covered by 150% of the prescription dose.

Discussion

The *American Brachytherapy Society* recommends that postimplant dosimetry be performed for all patients treated with permanent prostate brachytherapy, which is the current standard of care accepted by most brachytherapists (6, 7). As we perform real-time, US-based intraoperative planning and dosimetry, we obtained both US-based dosimetry and postimplant CT-based dosimetry. However, as our results show, several differences exist between intraoperative US-based dosimetry and postoperative CT-based dosimetry performed in the same patients.

Regarding rectal dose, we had already taken into account the fact that some dosimetric differences are seen between US plan and postimplant CT analyses (8, 9). Intraoperative US-based planning is performed with the probe in the rectum resulting in shape deformation compared to CT-based imaging. We tend to underestimate rectal dose on US-based dosimetry because of probe insertion. The volume of rectal wall receiving 145 Gy (rV_{100}) was thus restricted to <1.0 mL on US planning in most of our patients, and few of our patients experienced rectal adverse events (3). Although the rectum is differently contoured in US (anterior one-third of rectum) and CT (entire rectum), high dose area of rectal wall is restricted to a very small part of rectum near to the prostate. Thus, we consider that the difference of contouring between US and CT could not affect our data.

Although our results show that prostate volume on intraoperative US is almost the same as that on CT_1 (Table 2), prostate and urethral parameters on US-based dosimetry were significantly higher than those on CT_1-based dosimetry. This overestimation is not caused by prostate edema or hemorrhage. We assumed that the probe rotation angle for detecting a needle and seed would account for this overestimation (10). We usually implant seeds under real-time sagittal US. In intraoperative procedures, we tend to keep away from ring-down artifacts (11) and instead use more inner angles for chasing deposited locations of seeds. However, the very angles with artifact are actually the most accurate angles to detect the actual seeds and needles. We thus assumed that seed locations are tend to be recognized in more central portions of the prostate gland than actual locations, leading to the calculation of higher US parameters than CT parameters.

Whether US-based dosimetry or postoperative CT-based dosimetry is better able to predict patient outcome after prostate brachytherapy remains unclear. However, US-based dosimetry has potential difficulty predicting actual dosimetry because it is performed in a lithotomy position with anesthesia and needle insertion. In addition, considering the duration of 12 months for gamma-ray irradiation, intraoperative US represents a very limited and short-term status for the prostate. The *American Brachytherapy Society* recommendations of CT-based postimplant dosimetry remains the standard of care, and we believe this is a reasonable position to take.

Several authors have reported discrepancies between US and CT (12–16). Although some US-based parameters, such as pD_{90} might predict parameters of CT dosimetry, they reported other parameters provided only limited information. Our results also demonstrate significant differences between dosimetric parameters obtained by US, CT_1, and CT_{30}. Direct comparison between US and CT is therefore unacceptable. However, significant correlations exist between US and CT at least in prostate and urethral parameters. By comprehending the degree of difference, we might be able to make US planning more feasible.

Today, MRI becomes the gold standard for postimplant dosimetry in place of CT, if available. It is reported that the prostate contours determined by CT tend to be overestimated in comparison to the values determined by MRI; therefore, the DVH parameters of prostate determined by CT are tend to be underestimated (17). Further study, including MRI dosimetry is needed in the future.

Conclusion

Our results demonstrate significant differences between dosimetric parameters obtained by US and CT. However,

significant correlations also exist between US and CT, at least in prostate and urethral parameters. Clarification of the degrees of difference might make US planning more feasible.

References

[1] Battermann JJ, Boon TA, Moerland MA. Results of permanent prostate brachytherapy, 13 years of experience at a single institution. *Radiother Oncol* 2004;71:23–28.

[2] Potters L, Klein EA, Kattan MW, *et al.* Monotherapy for stage T1-T2 prostate cancer: Radical prostatectomy, external beam radiotherapy, or permanent seed implantation. *Radiother Oncol* 2004;71:29–33.

[3] Ishiyama H, Satoh T, Kitano M, *et al.* Four-year experience of interstitial permanent brachytherapy for Japanese men with localized prostate cancer. *Jpn J Clin Oncol* 2008;38:469–473.

[4] Cohen GN, Amols HI, Zelefsky MJ, *et al.* The Anderson nomograms for permanent interstitial prostate implants: A briefing for practitioners. *Int J Radiat Oncol Biol Phys* 2002;53:504–511.

[5] Rivard MJ, Coursey BM, Dewerd LA, *et al.* Update of AAPM Task Group No. 43 Report: A revised AAPM protocol for brachytherapy dose calculations. *Med Phys* 2004;31:633–674.

[6] Nag S, Beyer D, Friedland J, *et al.* American Brachytherapy Society (ABS) recommendations for transperineal permanent brachytherapy of prostate cancer. *Int J Radiat Oncol Biol Phys* 1999;44:789–799.

[7] Nag S, Bice W, DeWyngaert K, *et al.* The American Brachytherapy Society recommendations for permanent prostate brachytherapy postimplant dosimetric analysis. *Int J Radiat Oncol Biol Phys* 2000;46: 221–230.

[8]. Ishiyama H, Kitano M, Satoh T, *et al.* Difference in rectal dosimetry between pre-plan and post-implant analysis in transperineal interstitial brachytherapy for prostate cancer. *Radiother Oncol* 2006;78: 194–198.

[9] Pinkawa M, Asadpour B, Piroth MD, *et al.* Rectal dosimetry following prostate brachytherapy with strand seeds—Comparison of transrectal ultrasound intra-operative planning (day 0) and computed tomography-postplanning (day 1 vs. day 30) with special focus on sources placed close to the rectal wall. *Radiother Oncol* 2009;91:207-212.

[10] Ishiyama H, Kotani S, Satoh T, *et al.* Needle position during (125)I seed implantation: Accurately recognized by sagittal transrectal ultrasonography? *Radiat Med* 2008;26:512–515.

[11] Pfeiffer D, Sutlief S, Feng W, *et al.* AAPM Task Group 128: Quality assurance tests for prostate brachytherapy ultrasound systems. *Med Phys* 2008;35:5471–5489.

[12] Stone N, Hong S, Lo YC, *et al.* Comparison of intraoperative dosimetric implant representation with postimplant dosimetry in patients receiving prostate brachytherapy. *Brachytherapy* 2003;2:17–25.

[13] Ohashi T, Yorozu A, Toya K, *et al.* Comparison of intraoperative ultrasound with postimplant computed tomography—Dosimetric values at Day 1 and Day 30 after prostate brachytherapy. *Brachytherapy* 2007;6:246–253.

[14] Nag S, Shi P, Liu B, *et al.* Comparison of real-time intraoperative ultrasound-based dosimetry with postoperative computed tomography-based dosimetry for prostate brachytherapy. *Int J Radiat Oncol Biol Phys* 2008;70:311–317.

[15] Chauveinc L, Flam T, Solignac S, *et al.* Prostate cancer brachytherapy: Is real-time ultrasound-based dosimetry predictive of subsequent CT-based dose distribution calculation? A study of 450 patients by the Institute Curie/Hospital COCHIN (PARIS) Group. *Int J Radiat Oncol Biol Phys* 2004;59:691–695.

[16] Igidbashian L, Donath D, Carrier JF, *et al.* Poor predictive value of intraoperative real-time dosimetry for prostate seed brachytherapy. *Int J Radiat Oncol Biol Phys* 2008;72:605–609.

[17] Tanaka O, Hayashi S, Sakurai K, *et al.* Importance of the CT/MRI fusion method as a learning tool for CT-based postimplant dosimetry in prostate brachytherapy. *Radiother Oncol* 2006;81:303–308.

The Prostate 71:438 – 444 (2011)

Effect of a Phytotherapeutic Agent, Eviprostat®, on Prostatic and Urinary Cytokines/Chemokines in a Rat Model of Nonbacterial Prostatitis

Mikio Sugimoto,[1]* Michiko Oka,[2] Hiroyuki Tsunemori,[1] Motoki Yamashita,[1] and Yoshiyuki Kakehi[1]

[1]Department of Urology, Kagawa University Faculty of Medicine, Kagawa, Japan
[2]Discovery Research Laboratories, Nippon Shinyaku Co., Ltd, Kyoto, Japan

BACKGROUND. Chronic inflammation in the prostate has recently been recognized as an important component of the symptom progression of benign prostatic hyperplasia. The objective of this study was to evaluate a range of cytokines/chemokines in prostate tissue and urine to identify markers of prostate inflammation in a prostatitis model and to investigate the effect of a phytotherapeutic agent, Eviprostat®, on these markers.

METHODS. Ten-month-old male Wistar rats were divided into four groups. Nonbacterial prostatitis (NBP) was experimentally induced in groups 2–4 by castration followed by daily subcutaneous injection of 17β-estradiol for 30 days. Control rats were fed a standard diet, while animals in the Eviprostat groups were fed a diet containing 0.05 or 0.1% Eviprostat for 30 days. The levels of cytokines/chemokines in prostate tissue on the 31st day and in urine collected the day before castration and the day before removal of the prostate were determined.

RESULTS. Experimentally induced NBP increased the prostatic levels of the cytokines interleukin-1β (IL-1β) and tumor necrosis factor-α (TNF-α). The levels of the chemokines CCL2/monocyte chemoattractant protein-1 (MCP-1), CCL3/macrophage inflammatory protein-1α (MIP-1α), CXCL1/CINC-1, CXCL3/CINC-2, and CXCL5/LIX were elevated in both prostate and urine. Eviprostat significantly suppressed the increases in prostate IL-1β, TNF-α and CCL3/MIP-1α and prostatic and urinary CCL2/MCP-1 and CXCL1/CINC-1.

CONCLUSIONS. Chemokines, including CCL2/MCP-1 and CXCL1/CINC-1, were elevated in the prostate and urine of NBP rats, and Eviprostat potently suppressed the increases in CCL2/MCP-1 and CXCL1/CINC-1. These chemokines are therefore candidate diagnostic biomarkers for nonbacterial chronic prostatic inflammation. *Prostate 71: 438–444, 2011.*
© 2010 Wiley-Liss, Inc.

KEY WORDS: **rat nonbacterial prostatitis model; proinflammatory cytokines; chemokines; prostatic inflammation; benign prostatic hyperplasia; Eviprostat®**

INTRODUCTION

Benign prostatic hyperplasia (BPH) is a common proliferative disease characterized by nonmalignant enlargement of the prostate gland resulting from the excessive growth of epithelial and stromal cells [1]. BPH affects a growing number of older men and is often associated with bladder outlet obstruction and lower urinary tract symptoms (LUTS), which worsen the quality of life [2].

A recent report [3] suggests that chronic nonbacterial inflammation in the prostate plays a pivotal role in the symptom progression of BPH. Analysis of prostate biopsies in a subgroup of patients randomly selected from the Medical Therapy of Prostate Symptoms (MTOPS) study indicates that the presence of inflammatory infiltrates in the prostate of patients with BPH is

The authors have nothing to disclose.

*Correspondence to: Mikio Sugimoto, Department of Urology, Kagawa University Faculty of Medicine, Kita-gun, Kagawa 761-0793, Japan. E-mail: micsugi@med.kagawa-u.ac.jp
Received 6 August 2010; Accepted 26 September 2010
DOI 10.1002/pros.21299
Published online 28 October 2010 in Wiley Online Library (wileyonlinelibrary.com).

© 2010 Wiley-Liss, Inc.

associated with increased progression and a higher risk of acute urinary retention [4]. The Reduction by Dutasteride of Prostate Cancer Events (REDUCE) study demonstrated a significant correlation between BPH-associated prostate inflammation and LUTS [5]. We have previously demonstrated by gene-expression analysis of prostate tissue from patients with symptomatic BPH that the overexpression of various inflammation-related molecules is distinct from histological BPH [6] and that macrophage inhibitory cytokine-1, which is thought to inhibit macrophage activity, is significantly down-regulated in symptomatic BPH [7]. These findings support the hypothesis that molecular pathways involved in the development of inflammation in the prostate are activated in symptomatic BPH.

Chronic inflammatory infiltrates consisting mainly of activated T cells and macrophages are frequently found in BPH specimens on histological examination [8]. These infiltrating cells are responsible for the release of several kinds of cytokine/chemokine, which in turn leads to epithelial and stromal proliferation. Assessment of the cytokine/chemokine profile may give further insight into the mechanism of the progression of BPH and stimulate research into novel biomarkers of prostatic inflammation. Such biomarkers may help us identify patients at risk of developing BPH, diagnose prostate disease, and determine the efficacy of treatment for BPH symptoms. From a clinical viewpoint, noninvasive tests based on molecular markers in body fluids such as prostatic fluid or voided urine would be convenient and practical.

Although an appropriate animal model that mimics human BPH/LUTS/inflammation has not yet been established, some hormone-induced models produced by combined treatment with estradiol and testosterone or by treatment with estradiol alone in castrated rats have been proposed to be useful for elucidating the mechanisms of the molecular pathology of nonbacterial prostatitis (NBP) [9]. Combined treatment with estradiol and testosterone results in a significant increase in prostate weight and induces distinct prostatic stromal changes, although some reports show that testosterone, with its anti-inflammatory effect, attenuates the estradiol-induced increase in the incidence and severity of prostatitis [10]. On the other hand, treatment of castrated rats with estradiol alone causes a significant reduction in prostate weight, unlike human BPH. But this model is suitable for the investigation of prostatic inflammatory changes because it mimics human BPH with LUTS in several other respects, including an increased stromal-to-epithelial ratio and increased inflammatory infiltrates in the stroma [11]. Accordingly, by using a model of NBP induced in castrated aging rats by the injection of 17β-estradiol, we have previously observed increased production of interleukin-8 (IL-8) and tumor necrosis factor-α (TNF-α) in prostate tissue homogenates from NBP rats [12].

Eviprostat® is the most widely used phytotherapeutic agent for the treatment of BPH, having been prescribed for more than 40 years in Japan and Germany. Eviprostat is a mixture of five components: four are extracts from the umbellate wintergreen *Chimaphila umbellata*, the aspen *Populus tremula*, the small pasque flower *Pulsatilla pratensis*, and the field horsetail *Equisetum arvense*, and the fifth is wheat germ oil. Clinical studies show that treatment of BPH patients with Eviprostat improves the International Prostate Symptom Score (IPSS), quality of life score, and maximum and average urinary flow rates, decreases prostatic volume, and reduces inflammation in resected prostate specimens, without serious side effects [13,14].

Although the precise cellular mechanisms underlying the amelioration of BPH symptoms by Eviprostat remain to be clarified, Eviprostat treatment is reported to maintain low catecholamine levels and to inhibit pathological bladder activity in rats by decreasing adenosine triphosphate release from the bladder [15]. We have found that the components of Eviprostat have antioxidant and anti-inflammatory activity [16], while Eviprostat reduces increased oxidative stress and inflammation in the prostate and bladder in several rat models, resulting in an improvement in bladder function [12,17].

In the present study, we investigated cytokine/chemokine levels in the urine and inflamed prostate of NBP rats and the effect of Eviprostat on their levels.

MATERIALS AND METHODS

Animals

Ten-month-old male Wistar rats were supplied by Charles River Laboratories Japan (Yokohama, Japan). Rats were housed in individual cages in a room maintained at 20–26°C and a relative humidity of 35–75% with an alternating 12-hr light/dark cycle (the lights came on automatically at 8:00 a.m.). Food and water were freely given. The study was conducted in compliance with the Law for the Humane Treatment and Management of Animals (Law No. 105, 1 October 1973, as revised on 1 June 2006).

Induction of NBP in Aging Rats

Male rats were divided into groups of nine (groups 1 and 2) or ten (groups 3 and 4). The rats in group 1 (Sham) underwent sham castration and daily injection with sesame oil vehicle. The rats in the remaining groups were castrated and NBP was induced as previously described [9–11]. Briefly, rats were injected

subcutaneously with a daily dose of 0.25 mg/kg 17β-estradiol in 0.1 ml sesame oil for 30 days after the operation. During this time, rats in groups 1 (Sham) and 2 (NBP/Vehicle) were fed a standard diet (CE-2; Nihon Kurea, Osaka, Japan), while animals in the Eviprostat groups were fed the same diet containing either 0.05% Eviprostat (NBP/0.05% EVI) or 0.1% Eviprostat (NBP/0.1% EVI), prepared as previously described [15].

Determination of Cytokines/Chemokines in the Prostate

On the 31st day after castration, rats were anesthetized with pentobarbital (25 mg/kg, intraperitoneally) and the ventral prostates were rapidly removed. Cytokines/chemokines were determined as previously described [12,17]. Briefly, each prostate was homogenized in 10 volumes of ice-cold phosphate-buffered saline containing 200 μM phenylmethylsulfonyl fluoride as a protease inhibitor with a Physcotron Handy Micro Homogenizer (Niti-on, Tokyo, Japan). The homogenate was centrifuged at 30,000*g* for 60 min and cytokines/chemokines in the supernatant were determined by enzyme-linked immunosorbent assay (ELISA) with rat IL-1β, TNF-α, CXCL1/CINC-1, CXCL2/CINC-3, and CXCL3/CINC-2 kits from R&D Systems (Minneapolis, MN), rat CCL2/MCP-1 and CXCL5/LIX kits from RayBiotech (Norcross, GA), and a rat CCL3/MIP-1α kit from Koma Biotech (Seoul, Korea). Protein was determined by the Bradford method (Bio-Rad protein assay kit; Bio-Rad Laboratories, Tokyo, Japan) with bovine serum albumin as the standard protein.

Determination of Cytokines/Chemokines in Urine

The day before castration and again the day before removal of the prostate, urine was collected from the rats in a metabolic cage over a 24-hr period. The urine collected the day before castration (pre-urine) and the day before prostate removal (post-urine) was stored at −20°C to await processing. The urine was centrifuged at 1,200*g* for 5 min and the supernatant was used for the determination of cytokines/chemokines. Changes in urinary levels were obtained by subtracting pre-urine from post-urine levels.

Statistical Analysis

Data were analyzed with the SAS program (SAS/STAT, Ver. 8.2, SAS Institute, Cary, NC). Differences between Sham and NBP/Vehicle groups were analyzed for statistical significance by Student's *t*-test. To investigate the effects of Eviprostat in the NBP model, data for the Eviprostat-treated groups were analyzed by one-way analysis of variance and then by Dunnett's multiple-comparison test (two-tailed) against the NBP/Vehicle group.

RESULTS

The prostatic and urinary levels of the proinflammatory cytokines IL-1β and TNF-α, the CC chemokines CCL2/MCP-1 and CCL3/MIP-1α, and the CXC chemokines CXCL1/CINC-1, CXCL2/CINC-3, CXCL3/CINC-2, and CXCL5/LIX were measured. In the prostate, significant increases in the proinflammatory cytokines IL-1β and TNF-α (2.4- and 2.8-fold, respectively; Fig. 1), the CC chemokines CCL2/MCP-1 and CCL3/MIP-1α (2.9- and 17.4-fold, respectively; Fig. 2), and the CXC chemokines CXCL1/CINC-1, CXCL3/CINC-2, and CXCL5/LIX (3.9-, 2.3-, and 1.8-fold, respectively; Fig. 3) were observed in the NBP/Vehicle group compared to the sham-operated group. Only CXCL2/CINC-3 (Fig. 3B) was not significantly increased in the NBP/Vehicle group. A marked suppression of the increases in IL-1β and TNF-α (Fig. 1), as well as of the increases in the chemokines CCL2/MCP-1 and CCL3/MIP-1α (Fig. 2) and CXCL1/CINC-1 (Fig. 3A), was observed in the NBP/0.05% EVI and NBP/0.1% EVI groups. The suppression observed in the NBP/0.1% EVI group ranged from 71% for TNF-α to full suppression for IL-1β. The increases in CXCL3/CINC-2 and CXCL5/LIX (Fig. 3C,D) were not suppressed by Eviprostat treatment.

The urinary levels of both cytokines tested and one chemokine, CCL3/MIP-1α, were below detection limits in all animals. The levels of all other chemokines except for CXCL2/CINC-3 were significantly increased in the NBP/Vehicle group compared to the sham-operated group (Figs. 4 and 5). Eviprostat significantly attenuated the increases in CCL2/MCP-1 (Fig. 4) and CXCL1/CINC-1 (Fig. 5A) without significantly affecting the increases in CXCL3/CINC-2 or CXCL5/LIX (Fig. 5C,D).

DISCUSSION

Chronic prostatic inflammation, which is usually nonbacterial and asymptomatic, is an important component of symptom progression in patients with BPH. Cytokine/chemokine markers are desirable tools to predict symptom progression in human BPH/LUTS and to monitor the efficacy of treatment of BPH accompanied by chronic nonbacterial inflammation. The rat NBP model used in the present study is unique for its histological similarities to human BPH, including stromal predominance and the presence of inflammatory infiltrates surrounding the glandular structures. In this model, we have previously found that the concentrations of IL-8 and TNF-α in homogenates of

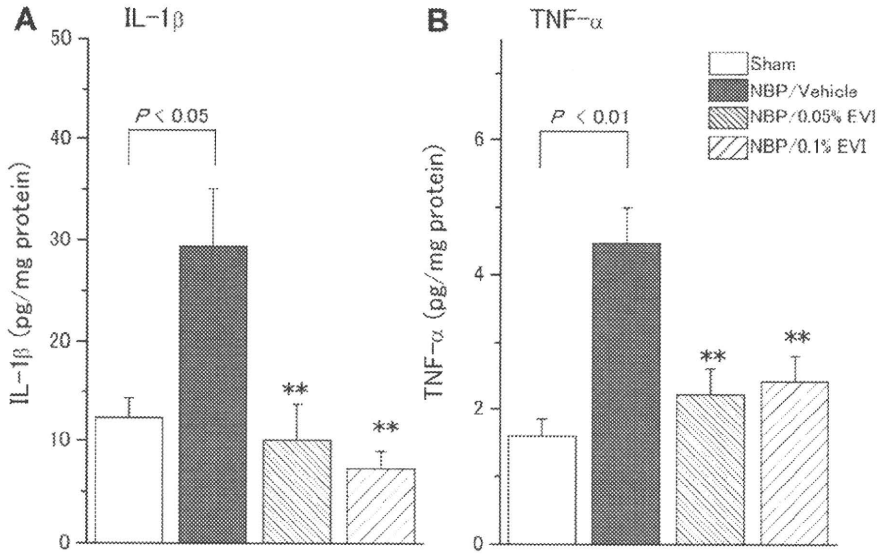

Fig. 1. Effect of Eviprostat on proinflammatory cytokine levels in the prostate of NBP rats. Prostates were removed on the 31st day after surgery and a cytosolic fraction was prepared for the determination of cytokines. Bars represent the mean ± SEM (n = 9 or 10). **P < 0.01 compared to the NBP/Vehicle group (Dunnett's multiple-comparison test).

prostatic tissue are significantly increased, and that the increases are suppressed by Eviprostat [12]. In the present study, we investigated cytokine/chemokine networks in the NBP rat prostate. We also investigated changes in the urinary expression profile of cytokines/chemokines in response to the anti-inflammatory medication Eviprostat in the hope of discovering one or more urinary markers that would be clinically useful for monitoring the treatment of asymptomatic prostatic inflammation in BPH.

Cytokines, including IL-1β and TNF-α, are regulatory proteins that are released by various cell types and that promote intercellular communication and immune responses. Chemokines such as CCL2/MCP-1, CCL3/MIP-1α, CXCL1/CINC-1, CXCL2/CINC-3, CXCL3/CINC-2, and CXCL5/LIX are chemotactic cytokines that recruit and activate immune cells at sites of inflammation. In the present study, the proinflammatory cytokines IL-1β and TNF-α and the chemokines CCL2/MCP-1, CCL3/MIP-1α, CXCL1/

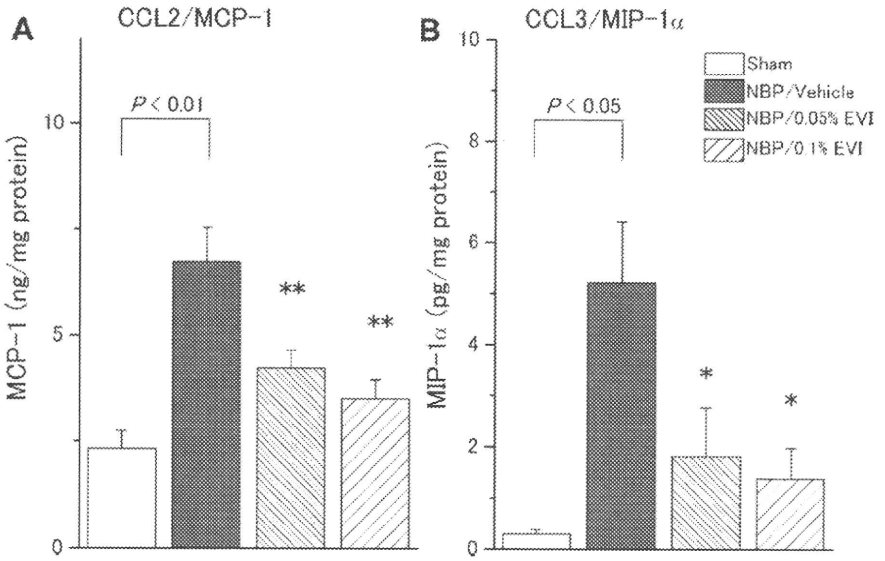

Fig. 2. Effect of Eviprostat on CC chemokine levels in the prostate of NBP rats. Prostates were removed on the 31st day after surgery and a cytosolic fraction was prepared for the determination of chemokines. Bars represent the mean ± SEM (n = 9 or 10). *P < 0.05, **P < 0.01 compared to the NBP/Vehicle group (Dunnett's multiple-comparison test).

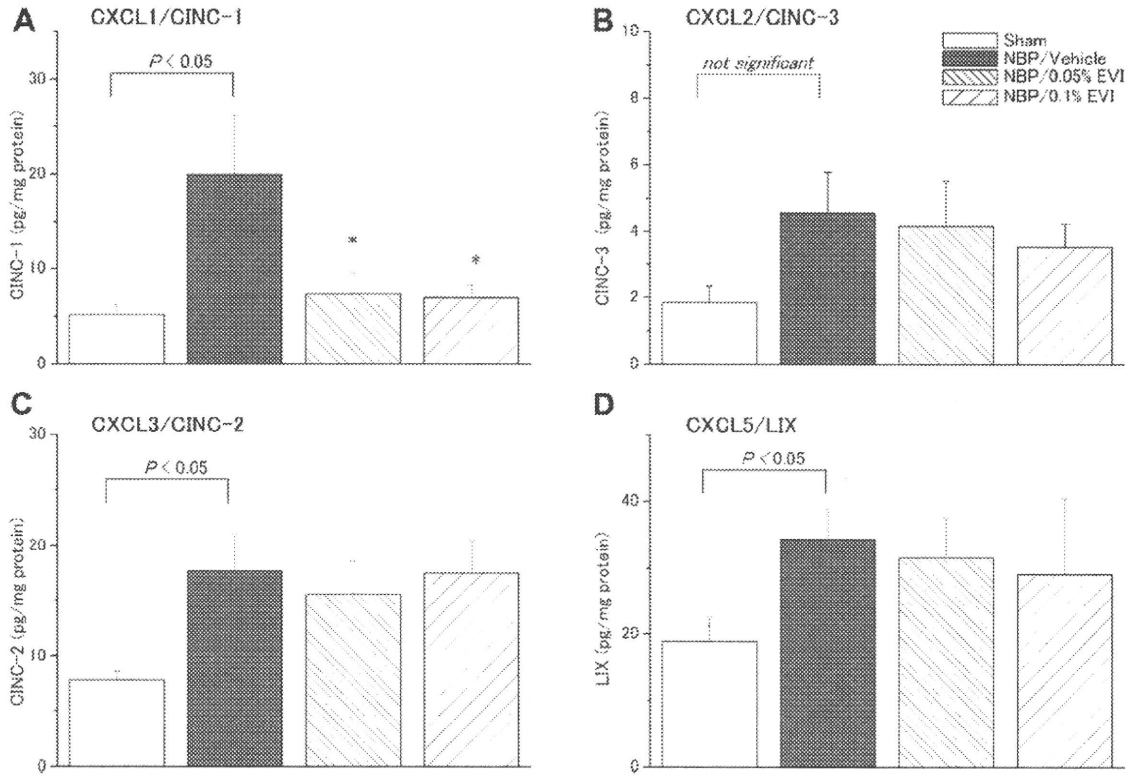

Fig. 3. Effect of Eviprostat on CXC chemokine levels in the prostate of NBP rats. Prostates were removed on the 31st day after surgery and a cytosolic fraction was prepared for the determination of chemokines. Bars represent the mean ± SEM (n = 9 or 10). *$P < 0.05$ compared to the NBP/Vehicle group (Dunnett's multiple-comparison test).

CINC-1, CXCL3/CINC-2, and CXCL5/LIX were significantly elevated in the inflamed prostate of NBP rats, although the role of each cytokine/chemokine in the inflamed prostate remains to be elucidated. Similarly,

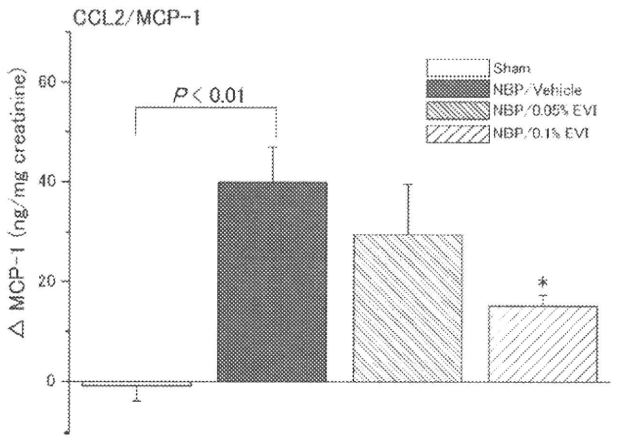

Fig. 4. Effect of Eviprostat on CCL2 (MCP-1) levels in the urine of NBP rats. Urine was collected over a 24-hr period the day before castration (pre-urine) and the day before removal of the prostate (post-urine). Bars represent the values obtained by subtracting pre-urine from post-urine levels (n = 9 or 10). *$P < 0.05$ compared with NBP/Vehicle (Dunnett's multiple-comparison test).

in urine from NBP rats, the chemokines CCL2/MCP-1, CXCL1/CINC-1, CXCL3/CINC-2, and CXCL5/LIX were elevated, although the two cytokines tested, as well as the chemokine CCL3/MIP-1α, were below detection limits.

CCL2/MCP-1 and CCL3/MIP-1α are members of the CC chemokine family. The former has specific chemotactic and activating activity toward lymphocytes and macrophages [18], while the latter is chemotactic for macrophages and T-cells [19]. Both chemokines have been suggested as possible markers for chronic prostatitis/chronic pelvic pain syndrome (CP/CPPS) [20]. We have now shown that in NBP rats CCL2/MCP-1 levels in both prostatic tissue and urine and CCL3/MIP-1α levels in prostatic tissue were significantly increased, though we did not detect urinary CCL3/MIP-1α. Fujita et al. [21] and Parsons et al. [22] have shown that prostatic CCL2/MCP-1 is a potential biomarker for LUTS associated with BPH. They demonstrated using prostate epithelial and stromal cell lines that CCL2/MCP-1 can be produced by prostatic stromal cells and that it stimulates prostate epithelial cell proliferation, an effect that can be blocked by CCL2/MCP-1 antagonists, providing evidence that CCL2/MCP-1 is a key mediator of BPH. CCL2/MCP-1

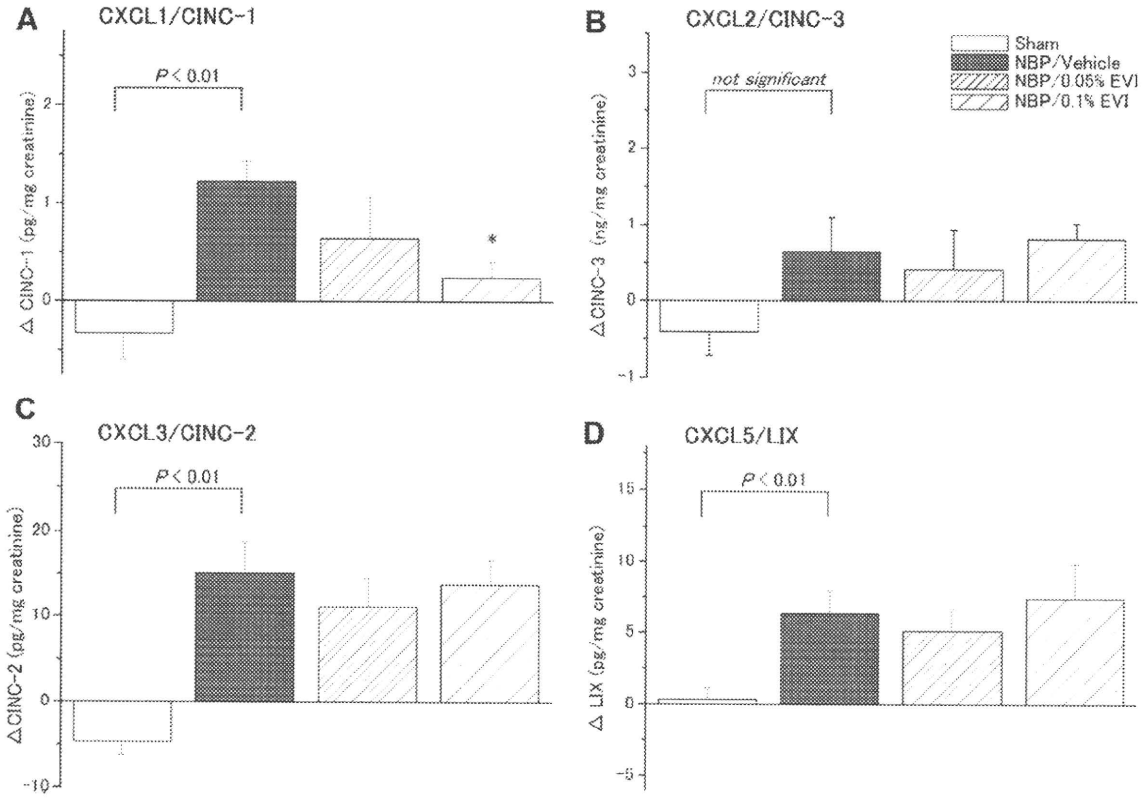

Fig. 5. Effect of Eviprostat on urinary CXC chemokine levels in the urine of NBP rats. See the legend of Figure 4 for details.

levels in prostatic secretions increase with prostate volume as well as macrophage numbers [21]. CCL2/MCP-1 levels in prostatic fluid are also significantly associated with high IPSS and severe LUTS [21].

CXCL1/CINC-1, CXCL2/CINC-3, CXCL3/CINC-2, and CXCL5/LIX belong to the CXC chemokine family. The IL-8-like chemokine CXCL1/CINC-1, which is secreted by multiple cell types, is a direct mediator of neutrophil accumulation and activation at inflammatory sites, and it may be responsible for the inflammatory reaction in the prostate. CXCL1/CINC-1 also recruits basophils and T cells and is a potent angiogenic factor [23]. In addition, elevated expression of IL-8 in the seminal plasma of patients with CP/CPPS and BPH is correlated with the symptom scores [24], while CXCL5/LIX, whose putative role is to activate and recruit neutrophils in inflammatory processes, is frequently elevated in the prostatic fluid of patients with CP/CPPS [25]. There are few studies on CXCL3/CINC-2, but this chemokine is reported to be produced by prostate stromal cells and to facilitate inflammatory responses [26].

Cytokines/chemokines in the prostatic fluid and seminal plasma of patients with CP/CPPS and BPH have been analyzed as possible biomarkers [20,24,27], and urinary CCL2/MCP-1 levels in BPH patients have been shown to be significantly associated with higher IPSS but not prostate volume [22]. In the present study, we found increased levels of the chemokines CCL2/MCP-1, CXCL1/CINC-1, CXCL3/CINC-2, and CXCL5/LIX in the prostate of NBP rats, and their levels were also increased in the urine. These chemokines may therefore be useful urinary markers of the grade and extent of inflammatory changes in the prostate of patients with CP/CPPS and BPH/LUTS.

In the inflamed prostate of NBP rats, Eviprostat significantly suppressed the increases in IL-1β, TNF-α, CCL2/MCP-1, CCL3/MIP-1α, and CXCL1/CINC-1 without affecting CXCL3/CINC-2 or CXCL5/LIX. Consistent with the results for prostate tissue, Eviprostat significantly suppressed the levels of CCL2/MCP-1 and CXCL1/CINC-1 in the urine. These results suggest that CCL2/MCP-1 and CXCL1/CINC-1 are promising urinary markers to predict responsiveness to anti-inflammatory agents. Furthermore, Eviprostat, which potently suppressed CCL2/MCP-1 and CXCL1/CINC-1 in the prostate, could be an effective treatment for chronic prostatic inflammation.

CONCLUSION

The increase in prostatic cytokine/chemokine levels observed in a rat model of NBP suggests that cytokine/chemokine cascades are crucial in the development of prostatic inflammation. In addition, certain cytokines/

chemokines that are elevated in both the urine and the prostate of these rats, including CCL2/MCP-1 and CXCL1/CINC-1, are promising urinary markers to predict responsiveness to anti-inflammatory agents.

REFERENCES

1. McVary KT. BPH epidemiology and comorbidities. Am J Manag Care 2006;12:S122–S128.
2. Berry SJ, Coffey DS, Walsh PC, Ewing LL. The development of human benign prostatic hyperplasia with age. J Urol 1984; 132:474–479.
3. Mishra VC, Allen DJ, Nicolaou C, et al. Does intraprostatic inflammation have a role in the pathogenesis and progression of benign prostatic hyperplasia? BJU Int 2007;100:327–331.
4. Roehrborn CG. Definition of at-risk patients: Baseline variables. BJU Int 2006;97(Suppl 2):7–11.
5. Nickel JC, Downey J, Young I, Boag S. Asymptomatic inflammation and/or infection in benign prostatic hyperplasia. BJU Int 1999;84:976–981.
6. Prakash K, Pirozzi G, Elashoff M, Munger W, Waga I, Dhir R, Kakehi Y, Getzenberg RH. Symptomatic and asymptomatic benign prostatic hyperplasia: Molecular differentiation by using microarrays. Proc Natl Acad Sci USA 2002;99:7598–7603.
7. Taoka R, Tsukuda F, Ishikawa M, Haba R, Kakehi Y. Association of prostatic inflammation with down-regulation of macrophage inhibitory cytokine-1 gene in symptomatic benign prostatic hyperplasia. J Urol 2004;171:2330–2335.
8. Theyer G, Kramer G, Assmann I, Sherwood E, Preinfalk W, Marberger M, Zechner O, Steiner GE. Phenotypic characterization of infiltrating leukocytes in benign prostatic hyperplasia. Lab Invest 1992;66:96–107.
9. Vykhovanets EV, Resnick MI, MacLennan GT, Gupta S. Experimental rodent models of prostatitis: Limitations and potential. Prostate Cancer Prostatic Dis 2007;10:15–29.
10. Naslund MJ, Strandberg JD, Coffey DS. The role of androgens and estrogens in the pathogenesis of experimental nonbacterial prostatitis. J Urol 1988;140:1049–1053.
11. Taniguchi S, Taoka R, Inui M, Sugimoto M, Kakehi Y. Influence of inflammation and aging on macrophage inhibitory cytokine-1 gene expression in rat ventral prostate. Urology 2009;73:410–414.
12. Oka M, Ueda M, Oyama T, Kyotani J, Tanaka M. Effect of the phytotherapeutic agent Eviprostat® on 17β-estradiol-induced nonbacterial inflammation in the rat prostate. Prostate 2009;69: 1404–1410.
13. Song Y, Li NC, Wang XF, Ma LL, Wan B, Hong BF, Na YQ. Clinical study of Eviprostat for the treatment of benign prostatic hyperplasia. Zhonghua Nan Ke Xue 2005;11:674–676 (in Chinese with English abstract).
14. Ishigooka M, Hashimoto T, Hayami S, Tomaru M, Nakada T, Mitobe K. Clinical and retrospective evaluation of Eviprostat: A non-hormonal and non-neuropharmacological agent for benign prostatic hyperplasia. Int Urol Nephrol 1995;27:61–66.
15. Sugaya K, Nishijima S, Tasaki S, Kadekawa K, Miyazato M, Ogawa Y. Mechanisms by which a phytotherapeutic drug influences bladder activity in rats. J Urol 2008;179:770–774.
16. Oka M, Tachibana M, Noda K, Inoue N, Tanaka M, Kuwabara K. Relevance of anti-reactive oxygen species activity to anti-inflammatory activity of components of Eviprostat, a phytotherapeutic agent for benign prostatic hyperplasia. Phytomedicine 2007;14:465–472.
17. Oka M, Fukui T, Ueda M, Tagaya M, Oyama T, Tanaka M. Suppression of bladder oxidative stress and inflammation by a phytotherapeutic agent in a rat model of partial bladder outlet obstruction. J Urol 2009;182:382–390.
18. Koch AE, Kunkel SL, Harlow LA, Johnson B, Evanoff HL, Haines GK, Burdick MD, Pope RM, Strieter RM. Enhanced production of monocyte chemoattractant protein-1 in rheumatoid arthritis. J Clin Invest 1992;90:772–779.
19. Koch AE, Kunkel SL, Harlow LA, Mazarakis DD, Haines GK, Burdick MD, Pope RM, Strieter RM. Macrophage inflammatory protein-1α. A novel chemotactic cytokine for macrophages in rheumatoid arthritis. J Clin Invest 1994;93:921–928.
20. Desireddi NV, Campbell PL, Stern JA, Sobkoviak R, Chuai S, Shahrara S, Thumbikat P, Pope RM, Landis JR, Koch AE, Schaeffer AJ. Monocyte chemoattractant protein-1 and macrophage inflammatory protein-1α as possible biomarkers for the chronic pelvic pain syndrome. J Urol 2008;179:1857–1861.
21. Fujita K, Ewing CM, Getzenberg RH, Parsons JK, Isaacs WB, Pavlovich CP. Monocyte chemotactic protein-1 (MCP-1/CCL2) is associated with prostatic growth dysregulation and benign prostatic hyperplasia. Prostate 2010;70:473–481.
22. Parsons JK, Fujita K, Ewing CM, Isaacs WB, Pavlovich CP. Prostatic monocyte chemotactic protein-1 (MCP-1): A novel biomarker for lower urinary tract symptoms associated with benign prostatic hyperplasia. J Urol 2009;181(Suppl):595.
23. Baggiolini M, Loetscher P, Moser B. Interleukin-8 and the chemokine family. Int J Immunopharmacol 1995;17:103–108.
24. Penna G, Mondaini N, Amuchastegui S, Degli Innocenti S, Carini M, Giubilei G, Fibbi B, Colli E, Maggi M, Adorini L. Seminal plasma cytokines and chemokines in prostate inflammation: Interleukin 8 as a predictive biomarker in chronic prostatitis/chronic pelvic pain syndrome and benign prostatic hyperplasia. Eur Urol 2007;51:524–533.
25. Hochreiter WW, Nadler RB, Koch AE, Campbell PL, Ludwig M, Weidner W, Schaeffer AJ. Evaluation of the cytokines interleukin 8 and epithelial neutrophil activating peptide 78 as indicators of inflammation in prostatic secretions. Urology 2000;56:1025–1029.
26. Kogan-Sakin I, Cohen M, Paland N, Madar S, Solomon H, Molchadsky A, Brosh R, Buganim Y, Goldfinger N, Klocker H, Schalken JA, Rotter V. Prostate stromal cells produce CXCL-1, CXCL-2, CXCL-3 and IL-8 in response to epithelia-secreted IL-1. Carcinogenesis 2009;30:698–705.
27. Nadler RB, Koch AE, Calhoun EA, Campbell PL, Pruden DL, Bennett CL, Yarnold PR, Schaeffer AJ. IL-1β and TNF-α in prostatic secretions are indicators in the evaluation of men with chronic prostatitis. J Urol 2000;164:214–218.

Published OnlineFirst February 9, 2010; DOI:10.1158/0008-5472.CAN-09-2984

Cancer Research

Identification of EP4 as a Potential Target for the Treatment of Castration-Resistant Prostate Cancer Using a Novel Xenograft Model

Naoki Terada, Yosuke Shimizu, Tomomi Kamba, et al.

Cancer Res 2010;70:1606-1615. Published OnlineFirst February 9, 2010.

Updated Version	Access the most recent version of this article at: doi:10.1158/0008-5472.CAN-09-2984
Correction	A correction to this article has been published. It is appended to this PDF and can also be accessed at: http://cancerres.aacrjournals.org/content/70/11/4785.full.pdf

Cited Articles	This article cites 47 articles, 22 of which you can access for free at: http://cancerres.aacrjournals.org/content/70/4/1606.full.html#ref-list-1
Citing Articles	This article has been cited by 1 HighWire-hosted articles. Access the articles at: http://cancerres.aacrjournals.org/content/70/4/1606.full.html#related-urls

E-mail alerts	Sign up to receive free email-alerts related to this article or journal.
Reprints and Subscriptions	To order reprints of this article or to subscribe to the journal, contact the AACR Publications Department at pubs@aacr.org.
Permissions	To request permission to re-use all or part of this article, contact the AACR Publications Department at permissions@aacr.org.

Downloaded from cancerres.aacrjournals.org on February 7, 2011
Copyright © 2010 American Association for Cancer Research

Published OnlineFirst February 9, 2010; DOI:10.1158/0008-5472.CAN-09-2984

Cancer Research

Therapeutics, Targets, and Chemical Biology

Identification of EP4 as a Potential Target for the Treatment of Castration-Resistant Prostate Cancer Using a Novel Xenograft Model

Naoki Terada[1], Yosuke Shimizu[1], Tomomi Kamba[1], Takahiro Inoue[1], Atsushi Maeno[1], Takashi Kobayashi[1], Eijiro Nakamura[1,6], Toshiyuki Kamoto[1,7], Toshiya Kanaji[8], Takayuki Maruyama[8], Yoshiki Mikami[2], Yoshinobu Toda[3], Toshiyuki Matsuoka[4], Yasushi Okuno[5], Gozoh Tsujimoto[5], Shuh Narumiya[4], and Osamu Ogawa[1]

Abstract

More effective therapeutic approaches for castration-resistant prostate cancer (CRPC) are urgently needed, thus reinforcing the need to understand how prostate tumors progress to castration resistance. We have established a novel mouse xenograft model of prostate cancer, KUCaP-2, which expresses the wild-type androgen receptor (AR) and which produces the prostate-specific antigen (PSA). In this model, tumors regress soon after castration, but then reproducibly restore their ability to proliferate after 1 to 2 months without AR mutation, mimicking the clinical behavior of CRPC. In the present study, we used this model to identify novel therapeutic targets for CRPC. Evaluating tumor tissues at various stages by gene expression profiling, we discovered that the prostaglandin E receptor EP4 subtype (EP4) was significantly upregulated during progression to castration resistance. Immunohistochemical results of human prostate cancer tissues confirmed that EP4 expression was higher in CRPC compared with hormone-naïve prostate cancer. Ectopic overexpression of EP4 in LNCaP cells (LNCaP-EP4 cells) drove proliferation and PSA production in the absence of androgen supplementation *in vitro* and *in vivo*. Androgen-independent proliferation of LNCaP-EP4 cells was suppressed when AR expression was attenuated by RNA interference. Treatment of LNCaP-EP4 cells with a specific EP4 antagonist, ONO-AE3-208, decreased intracellular cyclic AMP levels, suppressed PSA production *in vitro*, and inhibited castration-resistant growth of LNCaP-EP4 or KUCaP-2 tumors *in vivo*. Our findings reveal that EP4 overexpression, via AR activation, supports an important mechanism for castration-resistant progression of prostate cancer. Furthermore, they prompt further evaluation of EP4 antagonists as a novel therapeutic modality to treat CRPC. *Cancer Res; 70(4); 1606–15. ©2010 AACR.*

Introduction

Prostate cancer is one of the most frequently diagnosed cancers in the Western world (1). Because prostate cancer development is initially dependent on androgens, medical or surgical castration is the mainstay therapy for patients with advanced prostate cancer. However, most patients ultimately relapse after a period of initial response to this therapy, progressing to castration-resistant prostate cancer (CRPC). Effective therapeutic approaches for CRPC are extremely limited. Treatment with docetaxel was established as a new standard of care for CRPC patients (2). However, it is not curative, and optimal timing of administration remains controversial. Consequently, it is highly desirable to explore new therapeutic strategies based on detailed molecular mechanisms for the development of castration resistance in prostate cancer.

The generation of suitable *in vivo* models is critical to better understand the processes associated with the development and progression of prostate cancer. We have previously reported a novel prostate cancer xenograft model named KUCaP-1 (previously referred to as KUCaP; ref. 3). KUCaP-1 tumors harbor the W741C mutant androgen receptor (AR), regress soon after castration in mice, and do not regrow with long-term follow-up (4). We have now established another novel xenograft model named KUCaP-2 using locally recurrent CRPC specimens derived from a different patient. The KUCaP-2 tumors harbor wild-type AR, regress soon after castration, and restore their ability to proliferate after 1 to 2 months without AR mutation. As the sequential changes of the xenograft resemble the clinical behavior of prostate cancer, this model may provide an excellent system to

Authors' Affiliations: [1]Department of Urology, Kyoto University Graduate School of Medicine; [2]Department of Diagnostic Pathology, Kyoto University Hospital; [3]Anatomical Center, Kyoto University Graduate School of Medicine; [4]Department of Pharmacology, Faculty of Medicine, Kyoto University; [5]Department of Genomic Drug Discovery Science, Kyoto University Graduate School of Pharmaceutical Sciences, Kyoto, Japan; [6]Department of Medical Oncology, Dana-Farber Cancer Institute, Boston, Massachusetts; [7]Department of Urology, Miyazaki University, Miyazaki, Japan; and [8]Development Research Laboratories, Research Headquarters, Ono Pharmaceutical Co., Ltd., Osaka, Japan

Corresponding Author: Osamu Ogawa, Department of Urology, Kyoto University Graduate School of Medicine, 54, Shogoinkawahara-cho, Sakyo-ku, Kyoto 606-8507, Japan. Phone: 81-75-751-3325; Fax: 81-75-761-3441; E-mail: ogawao@kuhp.kyoto-u.ac.jp.

doi: 10.1158/0008-5472.CAN-09-2984

©2010 American Association for Cancer Research.

Downloaded from cancerres.aacrjournals.org on February 7, 2011
Copyright © 2010 American Association for Cancer Research

Published OnlineFirst February 9, 2010; DOI:10.1158/0008-5472.CAN-09-2984

study the mechanisms associated with castration-resistant progression of prostate cancer and to evaluate new treatment modalities for CRPC.

In KUCaP-2, prostaglandin E receptor EP4 subtype (EP4) expression significantly increased with the development of castration resistance. We explored the function of EP4 in prostate cancer cells as a potential target for the treatment of CRPC.

Materials and Methods

Generation of xenograft model. Clinical materials were used after informed consent was obtained, according to protocols approved by the institutional review board at Kyoto University Hospital. All experiments involving laboratory animals were done in accordance with the Guideline for Animal Experiments of Kyoto University. Local recurrent tumors after radical prostatectomy were resected trans-urethrally, minced into 20 to 30 mm^3 tumor bits, and transplanted s.c. into 5-wk-old male nude mice (Charles River Japan) with 50 μL of Matrigel (Becton Dickinson) injected around the implant. The KUCaP-2 xenograft was established ~10 mo after the first inoculation. The xenograft tumors were extracted and transplanted to several mice without Matrigel. Ninety percent of the tumor was serially transplantable.

Sequence analysis. Genomic DNA from the xenograft tissue was extracted and all of the exons of the *AR* gene were sequenced as previously reported (3).

Tissue sampling and DNA microarray analysis. The mice bearing KUCaP-2 tumors were castrated and the sequential changes in tumor volume were analyzed as previously reported (3). Serum samples were obtained at sacrifice to measure prostate-specific antigen (PSA) values. Xenograft tissues of KUCaP-2 were collected during various stages and total RNA was isolated and purified using the RNeasy Mini Kit (Qiagen). Changes in gene expression were analyzed using DNA microarray analysis with an Affymetrix Human Genome U133 Plus2.0.

Real-time PCR. cDNA was synthesized from total RNA using a First-Strand cDNA Synthesis Kit (Amersham Pharmacia Biotech). Real-time PCR was performed using SYBR green PCR Master Mix (Applied Biosystems) and monitored using GeneAmp 5700 (Applied Biosystems) in triplicate. The thermal cycling conditions were 95°C for 15 s, 60°C for 30 s, and 72°C for 30 s. The values were normalized to the levels of amplified glyceraldehyde-3-phosphate dehydrogenase (GAPDH). The sequences of primers were as follows: EP4, 5′-GGAAATGACCAGGCCAAGAC-3′ (sense) and 5′-CAACCCTGGACCTCACACCTA-3′ (antisense); PSA, 5′-GGAAATGACCAGGCCAAGAC-3′ (sense) and 5′-CAACCCTGGACCTCACACCTA-3′ (antisense); AR, 5′-CTTCACCAATGTCAACTCCA-3′ (sense) and 5′-TCATTCGGACACACTGGCTG-3′ (antisense); and GAPDH, 5′-GAATATAATCCCAAGCGGTTTG-3′ (sense) and 5′-ACTTCACATCACAGCTCCCC-3′ (antisense).

Antibodies and reagents. Anti-AR (C-19: sc-815) and anti-PSA (C-19: sc7638) antibodies were obtained from Santa Cruz Biotechnology. Anti-β-actin antibody (AC-15: ab6276) was purchased from Abcam. Anti-EP4 antibody (COOH terminus: 101775) for Western blotting was obtained from Cayman Chemical and anti-EP4 antibody (N terminus: LS-A3898) for immunohistochemistry was obtained from MBL International. The EP4-specific antagonist ONO-AE3-208 was provided by Ono Pharmaceutical Co. (5). 5α-Dihydrotestosterone was purchased from Sigma. Forskolin, an activator of adenylate cyclase, and dibutyryl cyclic AMP (dbcAMP), a cAMP analogue, were purchased from Nacalai Tesque. H-89, a cAMP-dependent protein kinase (PKA) inhibitor, was obtained from Biomol International. An expression vector, pcDNA3.1-EP4, was constructed by inserting the cDNA of human EP4, digested from a cloning vector, pBluescript-EP4 (6), into *Hin*dIII-*Bam*HI sites of pcDNA3.1(−). Vectors were transfected into the cells using Lipofectamine 2000 reagent (Invitrogen) and transfectants were selected by geneticin (Nacalai Tesque).

Western blotting and immunohistochemistry. Western blotting was performed with each primary antibody (AR, 1:400; PSA, 1:400; EP4 1:700; β-actin, 1:5,000) as previously reported (7). Immunohistochemistry was performed by standard indirect immunoperoxidase procedures using each primary antibody (AR, 1:100; PSA, 1:100; EP4 1:400), and the reaction was enhanced by microwave only in EP4 immunohistochemistry. Hormone-naïve prostate cancer (HNPC) tissues were derived from radical prostatectomy specimens of localized prostate cancer patients as tissue microarrays constructed as previously reported (8, 9). CRPC tissue samples were local tumors obtained from patients undergoing transurethral resection or autopsy. The expression intensity was graded as none, weak, moderate, and strong by a clinical pathologist (Y.M.) who was blind to the clinicopathologic data. The grading was determined based on the intensity of staining for at least 20% of the cancer cells.

Cell culture. The prostate cancer cell lines LNCaP, DU145, and PC3 were obtained from the American Type Culture Collection, passaged for fewer than 6 mo after resuscitation. The cells were routinely cultured in RPMI 1640 (Invitrogen) supplemented with 10% fetal bovine serum. For androgen-depleted conditions, cells were cultured in phenol red–free RPMI 1640 (Invitrogen) supplemented with 10% charcoal-stripped fetal bovine serum (CSFBS; Hyclone). To analyze the cell proliferation *in vitro*, 1.0×10^5 cells per well were seeded into six-well plates and grown for indicated days, and then cell numbers were counted in triplicate by a hemocytometer. For the assessment of *in vivo* tumor growth, 0.5×10^7 to 1.0×10^7 cells were inoculated with 100 μL Matrigel in the flank region of 5-wk-old male nude mice, and tumor volumes were measured once weekly.

RNA interference. AR knockdown was performed using stealth RNAi [stAR(1);HSS100620 and stAR(2);HSS100619] compared with control nonspecific stealth RNAi (stCtr;12935-400) purchased from Invitrogen. Cells were seeded at 5.0×10^5 per well in six-well plates and incubated for 24 h. Each 160 pmol of stealth RNAi was transfected using Lipofectamine 2000 reagent.

Luciferase assay. Cells were seeded at 1.5×10^5 per well in 24-well plates and were transiently cotransfected with 250 ng

Downloaded from cancerres.aacrjournals.org on February 7, 2011
Copyright © 2010 American Association for Cancer Research

Published OnlineFirst February 9, 2010; DOI:10.1158/0008-5472.CAN-09-2984

of pcDNA3.1-EP4, 250 ng of pGL3-PSAp-Luc, and 5 ng of pTK-RL using Lipofectamine 2000 reagent. After 24 h of incubation, the medium was changed to create androgen-depleted conditions and the cells were incubated again for 24 h. The luciferase activity of the cell lysate was measured using the Dual-Luciferase Reporter Assay System (Promega) with a luminometer (MicroLumat Plus LB96V, Berthold Technologies) in triplicate.

cAMP assay. Cells were seeded at 1.0×10^5 per well in 96-well plates and incubated for 24 h. Cells were washed once with PBS and cultured for 1 h in androgen-depleted conditions. The intracellular cAMP concentrations were assayed using the cAMP-EIA kit (RPN225; Amersham-Pharmacia Biotech) in duplicate. ONO-AE3-208 was added 10 min before the assay.

Statistical analysis. The data were expressed as mean ± SD and their statistically significant differences were determined by one-way ANOVA. Age, serum PSA levels, Gleason sums, and tumor volumes were compared by the Mann-Whitney *U* test, and EP4 staining levels were compared by the χ^2 test. Statistical analyses were all performed using SPSS software.

Results

KUCaP-2 is an androgen-dependent prostate cancer xenograft harboring wild-type AR, producing PSA, and developing castration resistance without AR mutation. Tumor tissues used for the establishment of KUCaP-2 were histologically diagnosed as prostate cancer based on positive AR and PSA immunohistochemistry staining (Fig. 1A). Western blotting analysis revealed that KUCaP-2 cells expressed AR and PSA (Fig. 1B). In mice, the KUCaP-2 tumor regressed soon after castration and reproducibly regrew after 1 to 2 months. Sequence analysis of *AR* in KUCaP-2 tumors before and after castration showed no *AR* mutation.

Xenograft tissues of KUCaP-2 were transplanted into 12 mice and collected during androgen-dependent growth (AD), castration-induced regression nadir (ND), and castration-resistant regrowth (CR) stages ($n = 4$, each; Fig. 1C). The tumor volumes were 3,012 ± 467, 562 ± 208, and 1,962 ± 560 mm^3, and the median PSA values of the mice were 166.0, 4.0, and 50.9 ng/mL for the AD, ND, and CR stages, respectively. There was no histologic difference among KUCaP-2 tumors of each stage (Fig. 1D, a–c). The nuclear expression levels decreased from the AD stage to the ND stage, indicating that the depletion of circulating androgen suppressed nuclear expression of AR in KUCaP-2 tumors at the ND stage. Nuclear expression recovered at the CR stage to levels similar to those at the AD stage (Fig. 1D, d–f).

EP4 expression was upregulated with the progression of castration resistance in KUCaP-2 tumors. To elucidate the mechanisms responsible for the development of castration resistance, we evaluated the gene expression profiles of tumors at each stage using DNA microarray analyses. In total, for 2,476 genes, there was a significant difference ($P < 0.05$) in expression between at least two stages. The *k*-means clustering ($k = 10$) of these genes was performed to select candidate genes (Fig. 2A). Previous reports on DNA microarray analysis in several different xenograft models showed that *AR* was the only gene consistently upregulated during castration-resistant progression (10). In our study, *AR* expression slightly increased from the AD stage to the ND stage (ratio = 2.7, $P = 0.006$), with no difference between the ND and CR stages (ratio = 1.1, $P = 0.280$). The *PSA* expression of tumors slightly and not significantly decreased from the AD stage to the ND stage (ratio = 0.6, $P = 0.138$) and recovered at the CR stage. To find genes associated with castration resistance, we explored genes in the cluster whose expression levels were low in both the AD and ND stages but high in the CR stage. Among 111 genes in this cluster, the CR/ND ratio of *EP4* expression was the highest (ratio = 15.7, $P = 0.029$; Table 1). These results were validated by real-time PCR analysis (Fig. 2B). Moreover, *EP4* expression was higher in the androgen-independent cell lines (DU145, PC3) compared with an androgen-dependent cell line (LNCaP; data not shown), consistent to other reports (11–13).

EP4 expression was higher in clinical CRPC than in HNPC. EP4 was mainly expressed in cellular membranes or in the cytoplasm of KUCaP-2 tumor cells, with more expression at the CR stage compared with the AD stage (Fig. 2C, a,b). Using KUCaP-2 samples from CR and AD stages as positive and negative controls, respectively, staining intensity of EP4 in clinical materials from 27 HNPC and 31 CRPC patients was graded (Fig. 2C, c–f). The characteristics of these patients were shown in Table 2. All the CRPC patients had PSA relapse. The serum PSA level and the Gleason sum were higher in CRPC than in HNPC. The EP4 expression level was significantly higher in CRPC than in HNPC ($P = 0.0001$).

EP4 overexpression induced castration-resistant progression of LNCaP cells through AR activation. We examined whether EP4 overexpression induced castration-resistant progression using LNCaP. LNCaP cells were stably transfected with pcDNA3.1-EP4, and two monoclonal EP4-overexpressing LNCaP clones were established and named LNCaP-EP4(A) and LNCaP-EP4(B). The EP4 signal activates adenylate cyclase, which results in acceleration of the production of cAMP (14). The intracellular cAMP concentrations, PSA expression levels, and cell proliferation ratio of LNCaP-EP4 without androgen were higher compared with those in vector alone–transfected LNCaP (LNCaP-mock) cells, indicating that overexpressed EP4 protein activated adenylate cyclase and induced PSA expression and cell proliferation without androgen (Fig. 3A).

To examine whether AR activation is associated with androgen-independent PSA expression and cell proliferation in LNCaP-EP4, AR expression was attenuated using a stealth RNAi system. PSA expression without androgen was suppressed more significantly by the attenuation of AR in LNCaP-EP4 cells than in LNCaP-mock cells. Further, the suppression of androgen-independent cell proliferation was statistically significant in LNCaP-EP4 cells, but not in LNCaP-mock cells, indicating that AR activation was associated with androgen independence of LNCaP-EP4 cells (Fig. 3B). We examined the effect of EP4 on AR activation using

Downloaded from cancerres.aacrjournals.org on February 7, 2011
Copyright © 2010 American Association for Cancer Research

Published OnlineFirst February 9, 2010; DOI:10.1158/0008-5472.CAN-09-2984

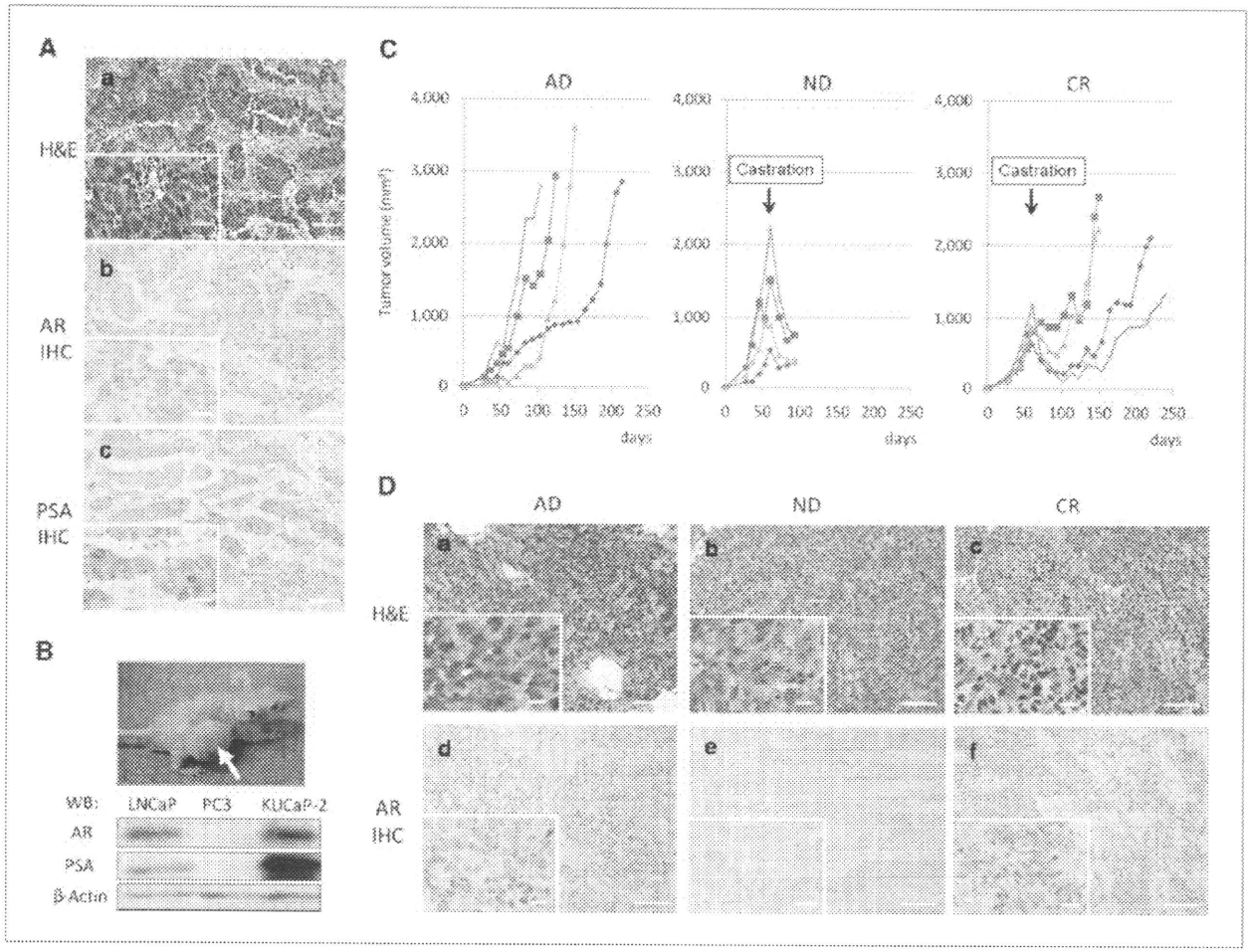

Figure 1. KUCaP-2, a novel established prostate cancer xenograft expressing AR and PSA, regresses after castration of mice and develops castration resistance with nuclear expression of AR. A, H&E staining (a), AR immunohistochemistry (IHC; b), and PSA immunohistochemistry (c) of tumor tissues used for the establishment of KUCaP-2. Scale bars, 50 μm, inset 5 μm. B, KUCaP-2 tumor (arrow, top) expressing AR and PSA detected with Western blotting (WB; LNCaP and PC3 presented as a positive and negative control; bottom). C, the sequential changes in xenograft tumor volume of KUCaP-2 before the tumor extraction at the AD, ND, and CR stages ($n = 4$ each). D, H&E staining (a–c), AR immunohistochemistry (d–f) at AD, ND, and CR stages of tumors. Scale bars, 50 μm, inset 5 μm.

a luciferase reporter assay in LNCaP cells. EP4 signaling promoted AR activation without androgen to ~50% of the level achieved with androgen stimulation and did not induce additional AR activation in the presence of androgen. Then, we examined whether the increase in cAMP levels and the acceleration of PKA activity was associated with AR activation. PSA expression in LNCaP cells without androgen was induced by both forskolin and dbcAMP but was inhibited by H-89 (Fig. 3C). These results indicate that the signal activation of EP4-cAMP-PKA-AR axis is associated with the castration resistance of LNCaP cells.

The castration of mice decelerated xenograft tumor growth in LNCaP-mock cells but not in LNCaP-EP4 cells (Fig. 3D). The serum PSA values of castrated mice bearing LNCaP-EP4 xenografts were significantly higher than those of mice bearing LNCaP-mock xenografts (median PSA at sacrifice: 4.0 and 32.5 ng/mL in LNCaP-mock and LNCaP-EP4 cells, respectively, $P < 0.05$). These results show that EP4 overexpression induces castration-resistant progression of LNCaP cells *in vivo*.

EP4 antagonist suppressed castration-resistant progression of LNCaP-EP4 and KUCaP-2 tumors. ONO-AE3-208 is an EP4-specific antagonist (5). The Ki values of ONO-AE3-208 for the prostanoid receptors are 1.3, 30, 790, and 2,400 nmol/L for EP4, EP3, FP, and TP, respectively, and >10,000 nmol/L for the other prostanoid receptors (15). To examine the EP4 antagonistic effect of ONO-AE3-208 on LNCaP-EP4 cells, intracellular cAMP concentrations were examined under a variety of ONO-AE3-208 concentrations in androgen-depleted conditions, indicating that 10 to 100 nmol/L of ONO-AE3-208 is sufficient to antagonize overexpressed EP4. This concentration of ONO-AE3-208 reached the Ki of EP3 and could also antagonize EP3. The EP3 signal inhibits adenylate cyclase, and thus the antagonism of EP3 increases intracellular cAMP concentrations (15). However, the suppression level of cAMP was proportional to the ONO-AE3-208 concentrations, suggesting

Downloaded from cancerres.aacrjournals.org on February 7, 2011
Copyright © 2010 American Association for Cancer Research

Published OnlineFirst February 9, 2010; DOI:10.1158/0008-5472.CAN-09-2984

that antagonistic effect against EP3 might be slight. The PSA expression of LNCaP-EP4 cells without androgen was also suppressed by the same concentrations of ONO-AE3-208 (Fig. 4A).

We then examined the *in vivo* antitumor effect of ONO-AE3-208. I.p. injection of ONO-AE3-208 (10 mg/kg; once a day) suppressed the castration-resistant growth of LNCaP-EP4 xenograft tumors (Fig. 4B). The serum PSA values of LNCaP-EP4 xenograft mice were also significantly decreased (median PSA at sacrifice: 5.7 and 3.7 ng/mL in controls and AE3-208, respectively, $P < 0.05$). The mean body weight of mice in the control and AE3-208 groups were almost the same, and no mice died during the treatment, indicating that ONO-AE3-208 was well tolerated at the concentrations used. The same dose of ONO-AE3-208 also suppressed the castration-resistant growth of KUCaP-2 tumors (Fig. 4C). The PSA production of KUCaP-2 tumors was significantly decreased (median PSA at sacrifice: 17.4 and 9.4 ng/mL in controls and AE3-208, respectively, $P < 0.05$). There were no significant differences in EP4 expression between the tumors of the control and AE3-208 groups (data not shown), indicating that ONO-AE3-208 antagonized EP4 without suppressing the receptor expression. In summary, EP4 antagonism with ONO-AE3-208 might be an effective and tolerable treatment modality for CRPC, in which EP4 overexpression induced castration-resistant progression (Fig. 4D).

Discussion

As CRPC is a heterogeneous group of diseases (16), many experimental models are required to elucidate the mechanisms for castration resistance. However, limited tissue availability for molecular studies and few available human prostate cancer cell lines with both AR- and androgen-dependent states have restricted prostate cancer research. Xenografts are models in which human tissue is transplanted into an immunodeficient mouse. In this way, human prostate cancer can be propagated *in vivo* for long periods to allow the study of tumor progression under different experimental hormonal conditions and to support the testing of novel therapies. Before 1993, only one prostate cancer xenograft, LNCaP

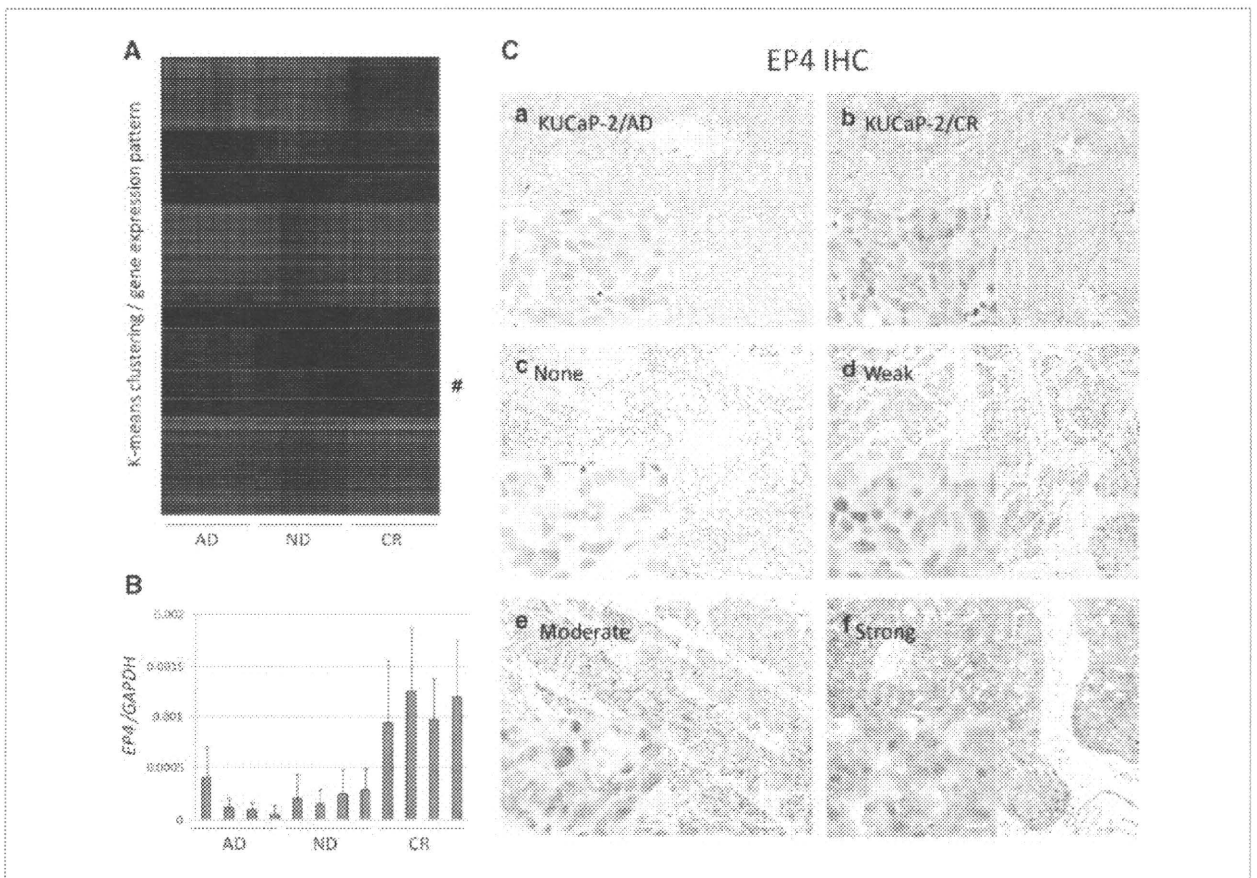

Figure 2. EP4 expression was upregulated during the castration-resistant progression of KUCaP-2. A, the *k*-means clustering of the DNA microarray data for AD, ND, and CR stage tumors of KUCaP-2. The *EP4* is in the cluster indicated with #. B, expression levels of *EP4* validated by real-time PCR analysis. C, the EP4 immunohistochemistry of AD stage (a) and CR stage (b) tumors of KUCaP-2. The staining intensity of EP4 in clinical samples of prostate cancer patients graded as none (c), weak (d), moderate (e) and strong (f). Scale bars, 50 μm, inset 5 μm.

Downloaded from cancerres.aacrjournals.org on February 7, 2011
Copyright © 2010 American Association for Cancer Research

Published OnlineFirst February 9, 2010; DOI:10.1158/0008-5472.CAN-09-2984

Table 1. Significantly upregulated genes at CR compared with AD and ND stages (10 highest CR/ND ratio)

Gene name (symbol)	CR/AD		CR/ND	
	Ratio	*P*	Ratio	*P*
Prostaglandin E receptor EP4 subtype (EP4)	15.7	0.01048	15.7	0.02903
Lumican (LUM)	23.6	0.00110	14.2	0.01095
Natriuretic peptide receptor C (NPRC)	2.3	0.19044	8.1	0.04921
N-methyl-D-aspartate 3A (GRIN3A)	9.1	0.00006	7.4	0.00029
Neuroligin 1 (NLGN1)	7.9	0.01844	6.1	0.04429
Coiled-coil domain containing 68 (CCDC68)	7.4	0.00013	4.4	0.00460
Tissue factor pathway inhibitor (TFPI)	4.1	0.04105	4.2	0.04678
Secretoglobin, family 1D, member 2 (LIPB)	8.2	0.01950	3.8	0.06641
Nudix-type motif 11 (UNDT11)	4.0	0.00444	3.7	0.01913
Eukaryotic translation initiation factor 1A Y-linked (EIF1AY)	2.6	0.07360	3.3	0.04354

(17), had been reported to be androgen dependent. LNCaP tumors shrink slightly after castration, usually with less than a 10% reduction in volume, and regrow less than 5 weeks after castration. Thereafter, several androgen-dependent xenografts have also been established. The LAPC-4 (18), LuCaP-23 (19), and PC346P (20) xenograft models reportedly show a response to castration similar to that of LNCaP. The CWR22 (21) and LAPC-9 (22) models showed recurrent growth after androgen ablation after 3 to 6 months, which was similar to our established xenograft, KUCaP-2. Similar to these models that mimic the clinical behavior of prostate cancer, KUCaP-2 may provide an excellent system to study the mechanisms associated with the castration-resistant progression of prostate cancer and help us develop novel treatment modalities against CRPC.

Most androgen-dependent xenografts were derived from patients with CRPC, as seen in KUCaP-2, because of the difficulty to obtain enough samples from patients with HNPC. It was suggested that prostate cancer contain a heterogeneous mixture of cells that vary in their dependence on androgen for growth and survival, and that treatment with androgen ablation therapy provides selective pressure and alters the relative concentration of these cells, thereby leading to the outgrowth of CRPC (22). These tumors presumably contain a mixture of growth-arrested, androgen-responsive tumor cells in addition to androgen-independent cells at the time of implantation into mice. In the androgenic environment of the intact male mouse, the androgen-responsive cells would gain a growth advantage and eventually develop into androgen-dependent xenografts.

The castration-resistant KUCaP-2 tumors expressed AR in their nuclei and produced PSA, suggesting that AR was activated with significantly low circulating androgen and is associated with the castration-resistant progression. Recent findings suggest that AR is an important transcription factor that mediates survival and proliferation signaling not only in HNPC but also in CRPC (23, 24). The androgen-independent activation of AR is mediated by several pathways (25, 26). The acquisition of mutations in *AR* is likely to be an important pathway (3, 27). However, KUCaP-2 harbors wild-type AR and progresses to castration resistance without AR mutation. Another possible pathway is its hypersensitivity to low levels

Table 2. Patient characteristics and EP4 staining grade in HNPC and CRPC

	HNPC	CRPC	*P*
Number	27	31	
Median serum PSA (ng/mL)	7.9 (3.8–31.3)	15.5 (0.5–949)	0.0066*
Median Gleason sum	7 (3–9)	9 (6–10)	0.0001*
EP4 staining grade†			0.0001‡
None	10 (37.0%)	5 (16.1%)	
Weak	17 (63.0%)	9 (29.1%)	
Moderate	0 (0%)	10 (32.2%)	
Strong	0 (0%)	7 (22.6%)	

*Mann-Whitney *U* test.
†The grading was determined on the intensity of staining for at least 20% of the cancer cells.
‡χ^2 test between HNPC and CRPC.

Downloaded from cancerres.aacrjournals.org on February 7, 2011
Copyright © 2010 American Association for Cancer Research

Published OnlineFirst February 9, 2010; DOI:10.1158/0008-5472.CAN-09-2984

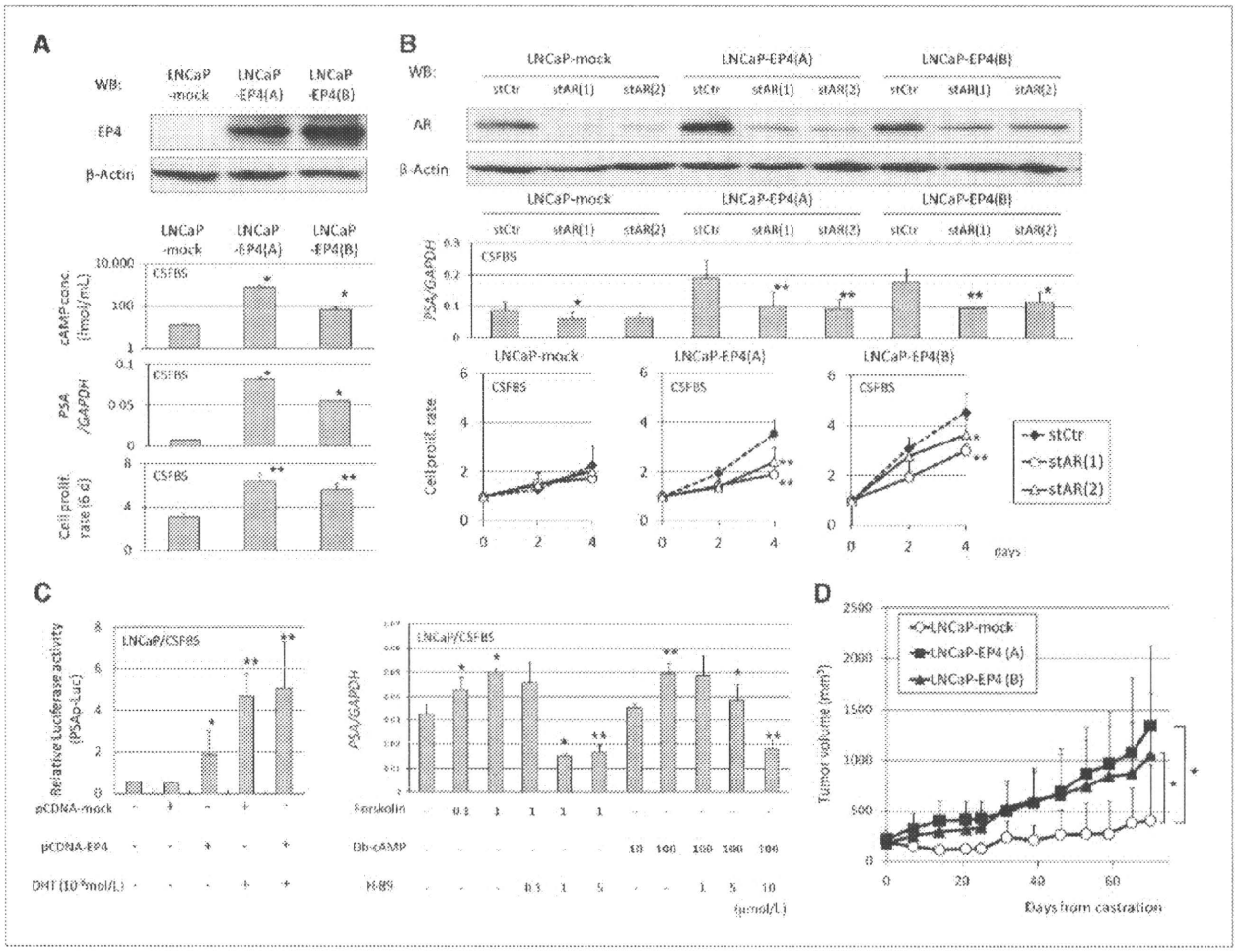

Figure 3. Overexpression of EP4 with cAMP-PKA signal activation promoted the castration-resistant progression of LNCaP cells through AR activation. A, EP4 protein expression detected with Western blotting in LNCaP-EP4(A) and LNCaP-EP4(B) compared with LNCaP-mock (top), intracellular cAMP concentrations, *PSA* expression, and cell proliferation ratio versus day 0 in androgen-depleted conditions (CSFBS) for 6 d (bottom). *, $P < 0.05$; **, $P < 0.005$ versus LNCaP-mock. B, AR expression attenuated using a stealth RNAi system detected with Western blotting (top), *PSA* expression levels on day 4 (middle), and cell proliferation ratio on days 2 and 4 versus day 0 (bottom) in CSFBS. *, $P < 0.05$; **, $P < 0.005$ versus LNCaP-mock. C, relative luciferase activities of PSAp-Luc in LNCaP cells with transfection of pcDNA3.1-mock and pcDNA3.1-EP4 in CSFBS and 5α-dihydrotestosterone (DHT) stimulation, respectively. *, $P < 0.05$; **, $P < 0.005$ versus control (left). PSA expression of LNCaP cells in CSFBS for 6 d under the administration of forskolin, dbcAMP, and H-89. *, $P < 0.05$; **, $P < 0.005$ versus preadministration (right). D, the sequential changes in xenograft tumor volume after the castration of mice (1×10^7 cells, $n = 5$ each). *, $P < 0.05$.

of androgens, induced by increased expression of the AR itself (10). In KUCaP-2, the *AR* mRNA expression slightly increased from the AD to ND and CR stages. However, the AR protein expression levels decreased at the ND stage and recovered at the CR stage to the same level as the AD stage both in the AR immunohistochemistry (Fig. 1D) and Western blotting (data not shown) analysis. One possible explanation for this discrepancy is that the AR protein might be degraded without androgen at ND stage and stabilized at the CR stage (28, 29). These results indicated that the upregulation of *AR* might merely be an adaptation of tumor cells to the condition of low androgen stimulation and not an essential indicator of castration-resistant progression. EP4 upregulation was observed during castration-resistant progression in KUCaP-2. EP4 expression was higher in clinical CRPC than in HNPC. The xenograft of EP4-overexpressing LNCaP cells developed castration resistance through AR activation. These results revealed that EP4 upregulation might lead to AR activation, resulting in the castration-resistant progression of prostate cancer. It was reported that the activation of a membrane-localized G protein-coupled receptor induced nuclear partition and activation of AR through the accumulation of intracellular cAMP and PKA activation (30). As EP4 is a G protein-coupled receptor, our data showing that EP4-cAMP-PKA axis activates AR are consistent to the report.

EP4 is one of the prostaglandin E2 (PGE2) receptors. PGE2, the product of cyclooxygenase-2 (COX-2) conversion of plasma membrane phospholipids, is the most common prostanoid and is associated with inflammatory disease (14) and cancer (31, 32). It was suggested that inflammation plays a

Downloaded from cancerres.aacrjournals.org on February 7, 2011
Copyright © 2010 American Association for Cancer Research

Published OnlineFirst February 9, 2010; DOI:10.1158/0008-5472.CAN-09-2984

role in prostate carcinogenesis (33, 34) and the regular consumption of non-steroidal anti-inflammatory drugs (NSAID) may reduce the risk of prostate cancer (35–37). Therefore, NSAIDs, including COX-2 inhibitors, have been tested in the treatment (38) and prevention (39) of prostate cancer. However, these approaches have met with limited success (40) and, sometimes, severe cardiovascular side effects (41), probably because COX-2 produces multiple products with pleiotropic effects in addition to PGE2. Therefore, targeting downstream signaling pathways of PGE2 may represent an attractive new strategy. There are four subtypes of PGE2 receptors, EP1 to EP4. The intracellular signaling differs among the receptor subtypes; EP1 is coupled to calcium mobilization, EP3 inhibits adenylate cyclase, and EP2 and EP4 stimulate adenylate cyclase in various types of cells (42). The effects of PGE2 are dependent on the ligand concentration and the target cell receptor expression (32). Experimental studies have suggested that increased EP2 and EP4 expression is important during colorectal and prostate cancer progression (43, 44). In KUCaP-2, EP2 expression did not increase significantly during castration-resistant progression (data not shown), indicating that EP4 might be more strongly associated with castration resistance than EP2 in this model. To examine the association of PGE2 and cancer progression, the serum PGE2 concentrations of mice bearing KUCaP-2 were examined by PGE2 Express EIA kit (500141; Cayman Chemical). Unfortunately, reproducible results could not be obtained, probably because of the instability of PGE2.

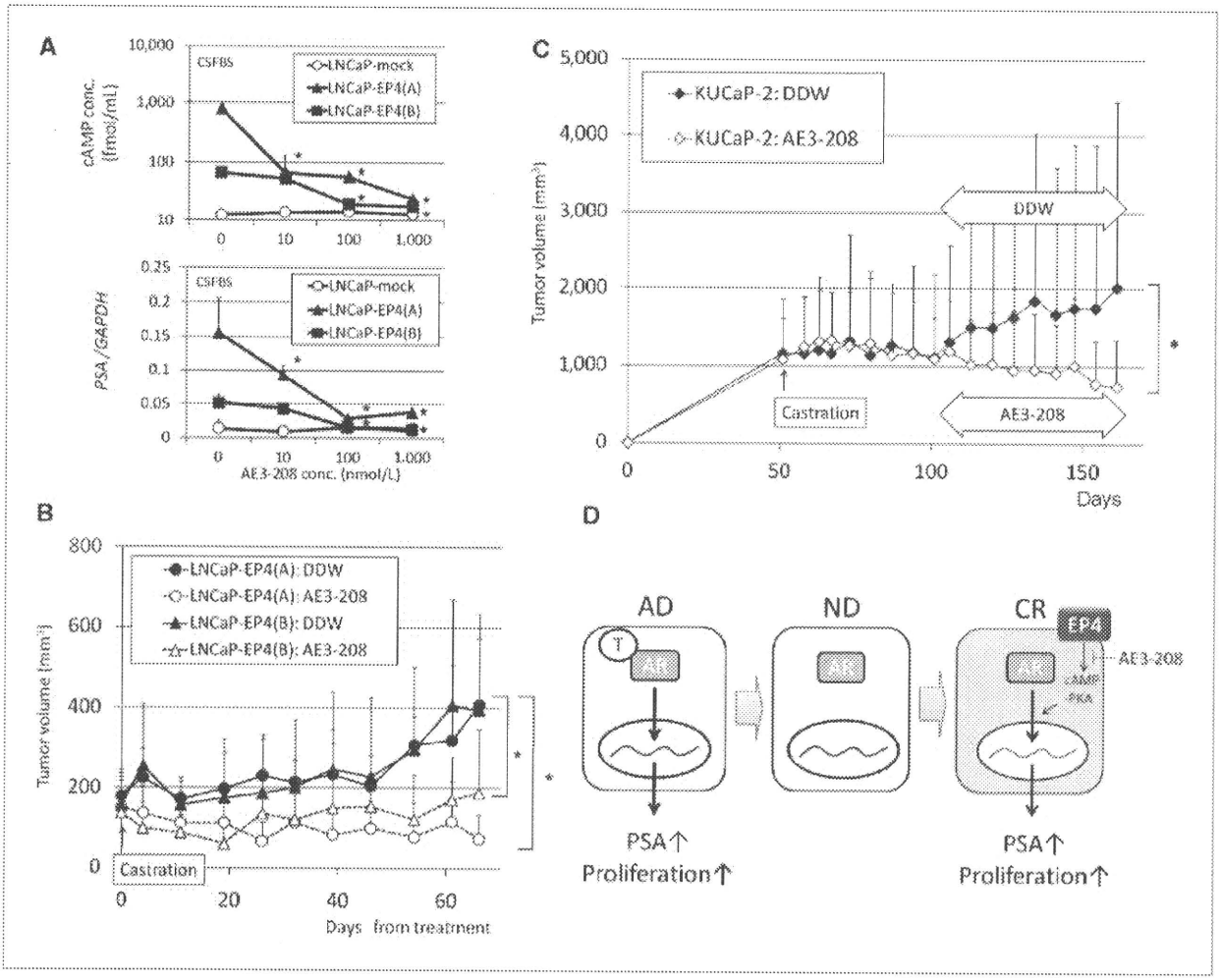

Figure 4. Castration-resistant progression of LNCaP-EP4 and KUCaP-2 was suppressed by ONO-AE3-208 treatment. A, the cAMP concentration (top) and *PSA* expression (bottom) of LNCaP-mock, LNCaP-EP4(A), and LNCaP-EP4(B) under the *in vitro* administration of ONO-AE3-208 in CSFBS. *, $P < 0.05$ versus LNCaP-mock. B, the sequential changes in LNCaP-EP4(A) and LNCaP-EP4(B) xenograft tumors treated with i.p. injection of 200 μL/d distilled water (DDW) and 10 mg/kg/d ONO-AE3-208 (AE3-208) started soon after the castration of mice and continued for 70 d (0.5×10^7 cells, $n = 5$ each). *, $P < 0.05$. C, the sequential changes in KUCaP-2 tumors treated with the same volume of DDW and AE3-208 solution started 50 d after castration and continued for 60 d ($n = 5$ each). *, $P < 0.05$. D, schematic representation of the relationship between EP4 overexpression and castration resistance. After castration, the upregulated EP4 induces activation of the AR without androgen and promotes castration-resistant cell proliferation and PSA production, which is suppressed by ONO-AE3-208 administration. T, androgen.

Downloaded from cancerres.aacrjournals.org on February 7, 2011
Copyright © 2010 American Association for Cancer Research

Published OnlineFirst February 9, 2010; DOI:10.1158/0008-5472.CAN-09-2984

Therefore, it might be difficult to examine the serum PGE2 concentrations in clinical samples. The secreted PGE2 concentrations in LNCaP-EP4 cells were higher than in LNCaP-mock cells [20.3 ± 15.4, 48.7 ± 4.9, and 44.7 ± 11.5 pg/mL in LNCaP-mock, LNCaP-EP4(A), and LNCaP-EP4(B), respectively]. However, the administration of PGE2 into LNCaP-EP4 could not induce cell proliferation and PSA production. To elucidate the association of PGE2 and cancer progression needs further examinations.

The cell proliferation of LNCaP-EP4 was significantly higher than that of LNCaP-mock under androgen-depleted medium but not under normal medium (data not shown), indicating that EP4 overexpression enhanced androgen-independent but not androgen-dependent proliferation of LNCaP cells *in vitro*. However, the *in vivo* tumor growth of LNCaP-EP4 was significantly higher than that of LNCaP-mock in intact mice (193 ± 76 and 121 ± 46 mm^3 on day 30, respectively, $P = 0.003$). Moreover, the xenograft tumor take-up rate of LNCaP-EP4 was higher than that of LNCaP-mock (~100% and 60%, respectively). It was reported that PGE2 regulated angiogenesis in PC3 cells through EP2 and EP4 (44). Therefore, it was suggested that EP4 overexpression might increase cell proliferation of LNCaP cells *in vivo* through angiogenesis. The PSA expression of LNCaP-EP4 was significantly higher than that of LNCaP-mock under androgen-depleted medium. Although EP4 expression was higher in LNCaP-EP4(B) than in LNCaP-EP4(A), the intracellular cAMP concentration and PSA expression levels were higher in LNCaP-EP4(A) than in LNCaP-EP4(B). To investigate the reasons for the discrepancy, we performed transient transfection analyses with several different amounts of pcDNA3.1-EP4. The PSA expression levels were correlated with EP4 expression levels in LNCaP cells transiently transfected with the EP4 expression vector, suggesting that the reasons for this discrepancy might be clonal variations of LNCaP-EP4 (data not shown). The expression of TMPRSS2, one of other AR-regulated genes (45), was also increased with EP4 overexpression and decreased by the attenuation of AR (data not shown). These results indicated that EP4 may increase PSA expression partly in an AR-dependent manner; however, we do not exclude possibilities that EP4 increases PSA and TMPRSS2 expressions through an AR-independent manner. Analysis of these mechanisms needs further investigations.

It was suggested that the EP4-cAMP-PKA axis can activate the β-catenin/TCF signaling pathway, leading to cancer progression (46), and that the EP4-specific antagonist, ONO-AE3-208, inhibits the progression of EP4-expressing colorectal cancer (47, 48). The present study is the first report showing that ONO-AE3-208 reduces the castration-resistant progression of prostate cancer cells induced by EP4 overexpression. ONO-AE3-208 did not suppress the proliferation of KUCaP-2 in intact mice (data not shown), suggesting that EP4 antagonism might have no antitumor effect against HNPC. DU145 and PC3 are AR-negative prostate cancer cells with high EP4 expression. The *in vitro* administration of 100 nmol/L ONO-AE3-208 decreased intracellular cAMP concentrations of these cells. However, it did not suppress their cell proliferation *in vitro* and *in vivo* (data not shown). It was suggested that the EP4-cAMP-PKA axis might not be associated with their cell proliferation.

In conclusion, we found that EP4 overexpression is one of the mechanisms responsible for progression to CRPC using a novel xenograft model KUCaP-2. The administration of EP4 antagonist *in vivo* suppressed the castration-resistant progression of KUCaP-2, indicating that EP4 may be a potential target for the treatment of CRPC.

Disclosure of Potential Conflicts of Interest

No potential conflicts of interest were disclosed.

Acknowledgments

We thank Tomoko Kobayashi and Megumi Kishida for their valuable technical assistance.

Grant Support

Grants-in-aid for scientific research from the Ministry of Education, Culture, Sports, Science and Technology of Japan.

The costs of publication of this article were defrayed in part by the payment of page charges. This article must therefore be hereby marked *advertisement* in accordance with 18 U.S.C. Section 1734 solely to indicate this fact.

Received 8/11/09; revised 11/30/09; accepted 12/2/09; published OnlineFirst 2/9/10.

References

1. Gronberg H. Prostate cancer epidemiology. Lancet 2003;361:859–64.
2. Petrylak DP, Tangen CM, Hussain MH, et al. Docetaxel and estramustine compared with mitoxantrone and prednisone for advanced refractory prostate cancer. N Engl J Med 2004;351:1513–20.
3. Yoshida T, Kinoshita H, Segawa T, et al. Antiandrogen bicalutamide promotes tumor growth in a novel androgen-dependent prostate cancer xenograft model derived from a bicalutamide-treated patient. Cancer Res 2005;65:9611–6.
4. Terada N, Shimizu Y, Yoshida T, et al. Antiandrogen withdrawal syndrome and alternative antiandrogen therapy associated with the W741C mutant androgen receptor in a novel prostate cancer xenograft. Prostate. Epub 2009.
5. Kabashima K, Sakata D, Nagamachi M, Miyachi Y, Inaba K, Narumiya S. Prostaglandin E2-4 signaling initiates skin immune responses by promoting migration and maturation of Langerhans cells. Nat Med 2003;9:744–9.
6. Bastien L, Sawyer N, Grygorczyk R, Metters KM, Adam M. Cloning, functional expression, and characterization of the human prostaglandin E2 receptor EP2 subtype. J Biol Chem 1994;269:11873–7.
7. Inoue T, Yoshida T, Shimizu Y, et al. Requirement of androgen-dependent activation of protein kinase Cζ for androgen-dependent cell proliferation in LNCaP cells and its roles in transition to androgen-independent cells. Mol Endocrinol 2006;20:3053–69.
8. Inoue T, Segawa T, Shiraishi T, et al. Androgen receptor, Ki67, and p53 expression in radical prostatectomy specimens predict treatment failure in Japanese population. Urology 2005;66:332–7.
9. Shimizu Y, Segawa T, Inoue T, et al. Increased Akt and phosphorylated Akt expression are associated with malignant biological features of prostate cancer in Japanese men. BJU Int 2007;100:685–90.

Downloaded from cancerres.aacrjournals.org on February 7, 2011
Copyright © 2010 American Association for Cancer Research